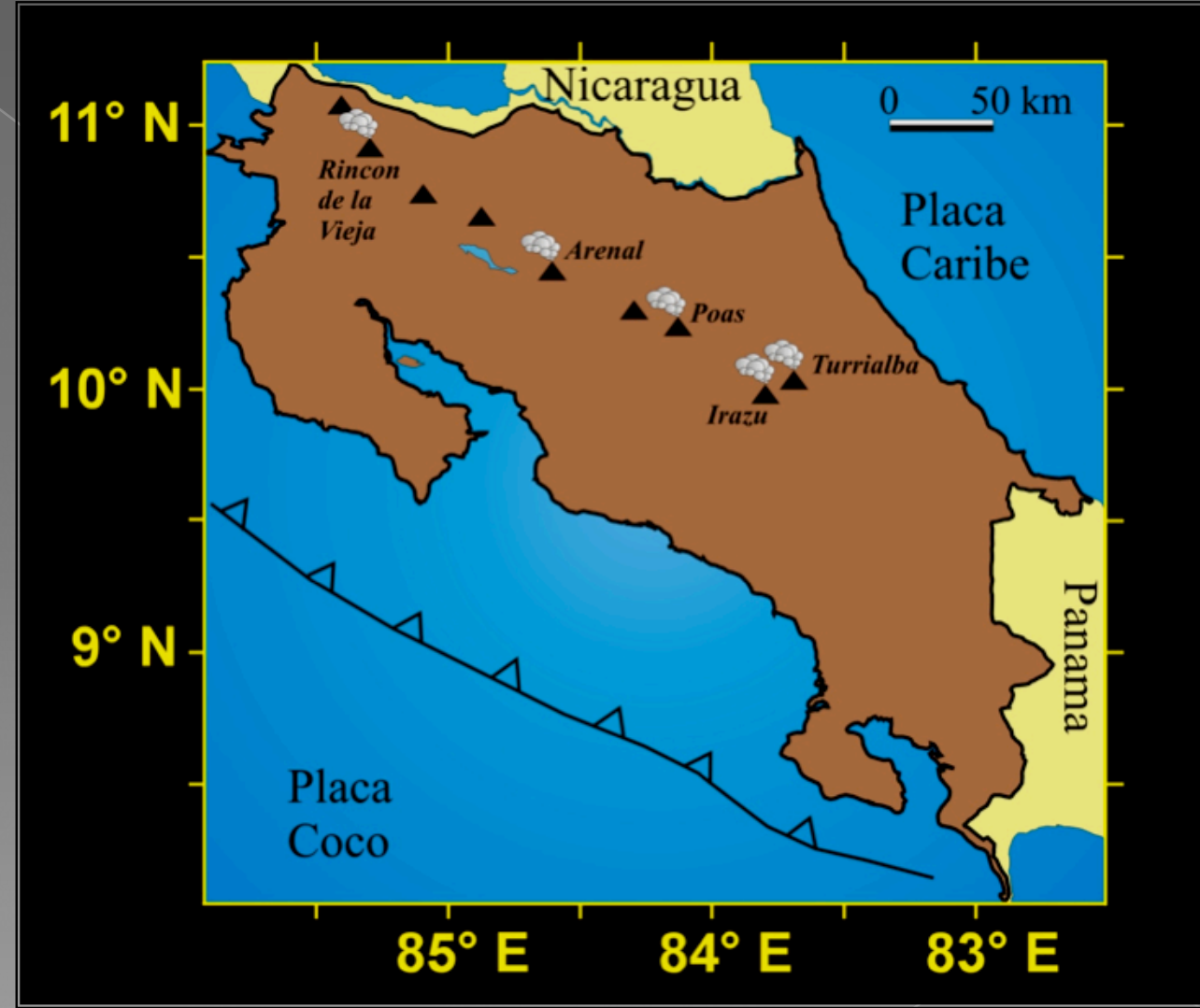
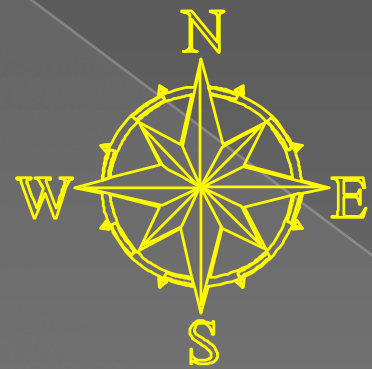


PASI 2011
Open Vent Volcano Hazards Workshop

**Case studies – application of techniques
and interpretation of data**

Arenal, Turrialba and Poas volcanoes

Mauricio Mora Fernández
Escuela Centroamericana de Geología
Universidad de Costa Rica



ARENAL VOLCANO



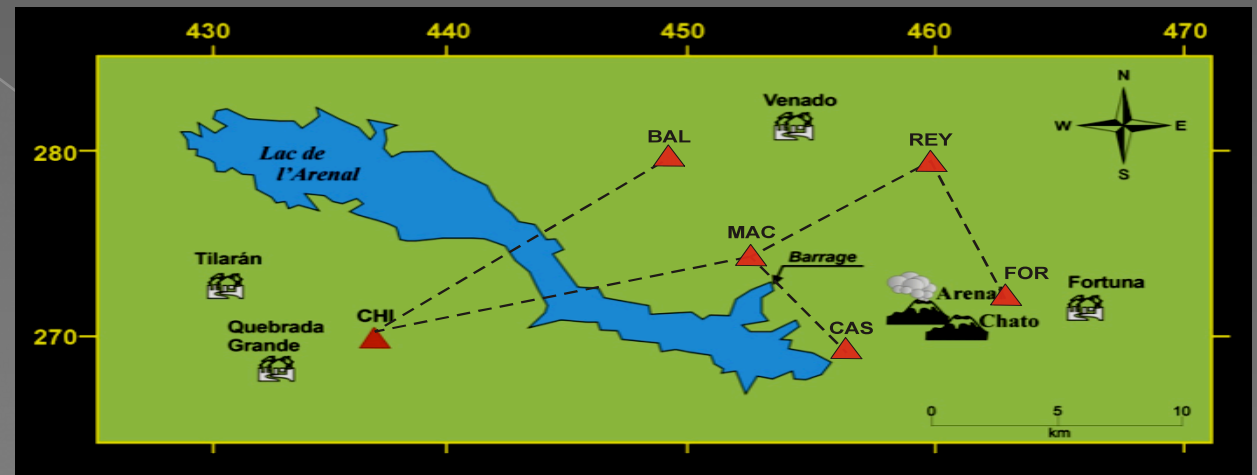
Seismological studies at Arenal



Topic	References
Classification, description, monitoring	Matumoto, 1968 Minakami et al., 1969 Matumoto, 1976 Montero, 1984 Alvarado et al., 1987 Morales et al., 1988 Alvarado et al., 1988 Melson, 1989 Barboza & Melson, 1990 Soto et al., 1990 Mora, 1991 Barquero et al., 1992 Métaxian et al., 1996 Alvarado et al., 1997 Benoit et al., 2003
Seismic source	Benoit & McNutt, 1997 Hagerty et al., 1997 Hagerty, 1998 Garcés et al., 1998 Hagerty et al., 2000 Mora, 2003 Lesage et al., 2006
Localization of events	Alvarado et al., 1997 Hagerty et al., 2000 Métaxian et al., 2002
Structure of volcanic edifice	Métaxian et al., 1996 Leandro et al., 1999 Mora et al., 2001 Mora et al., 2004

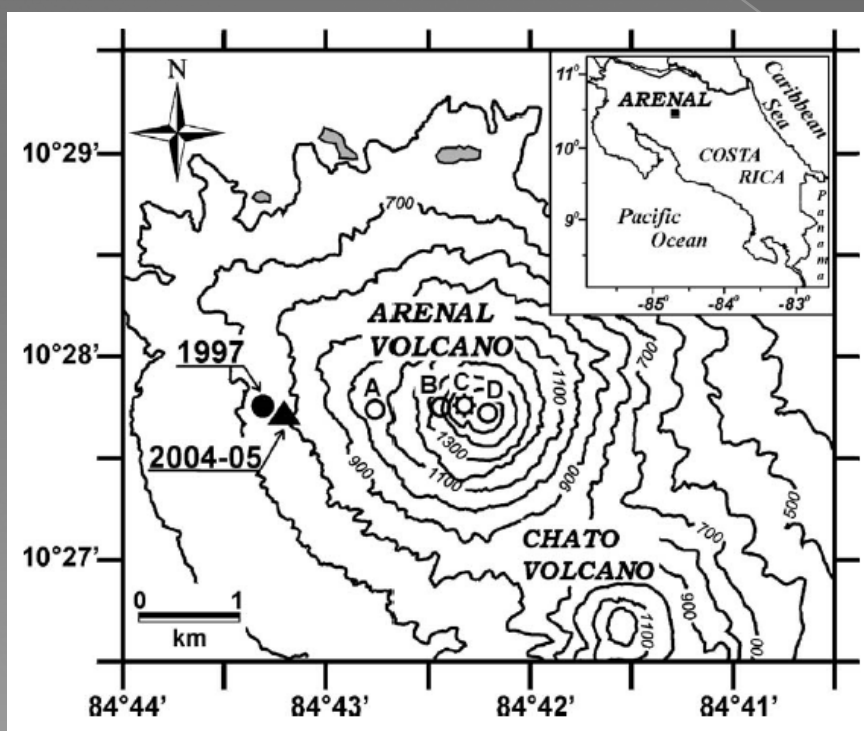
1. Monitoring system

Observatorio Sismológico y Vulcanológico de Arenal y Miravalles
(OSIVAM)



OSIVAM (Chiripa, Tilarán)

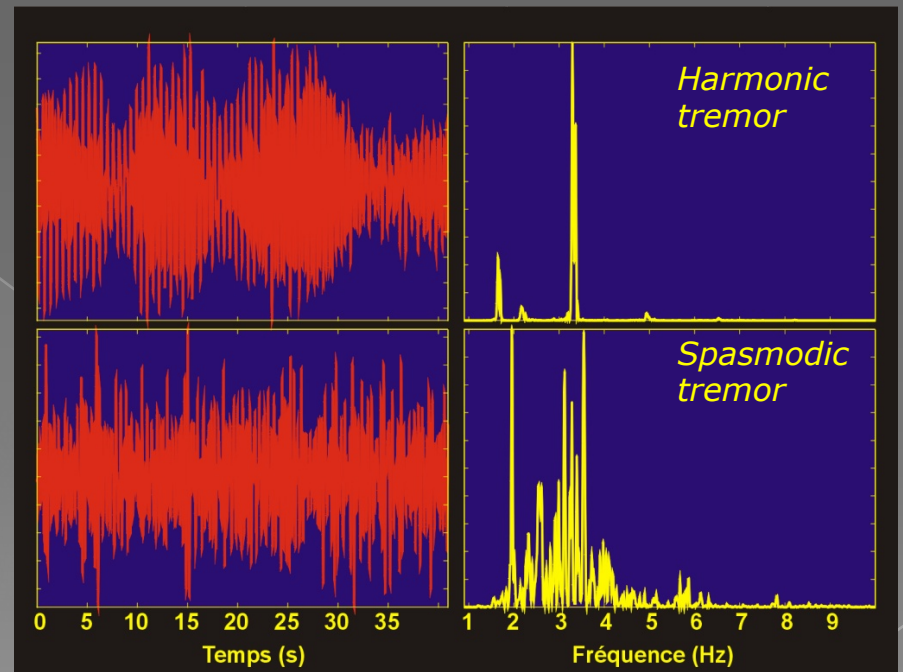
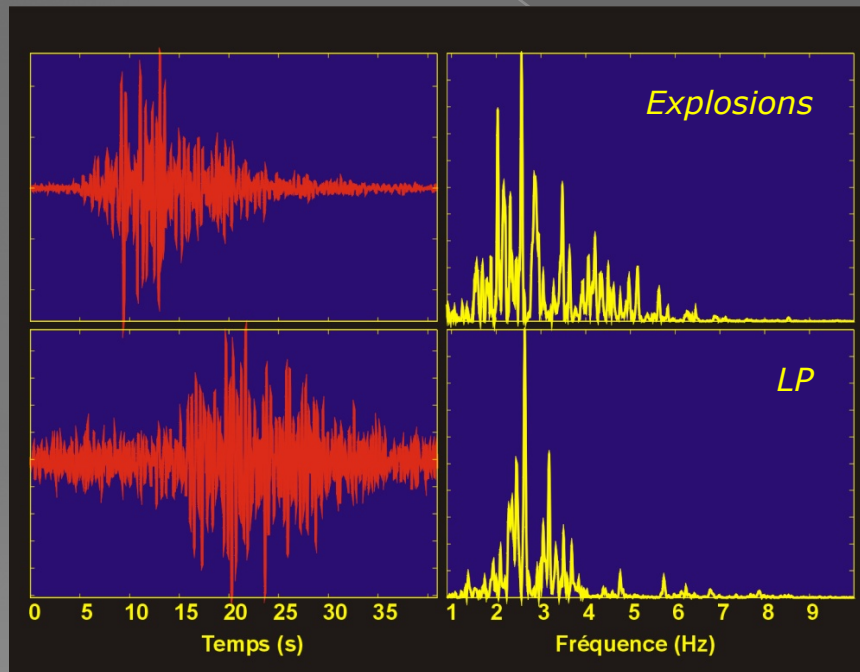
- Town.
- Volcanic edifice.
- Telemetric link.
- Seismic station.



December 2003

2. Classification of seismic signals:

Four basic type of events:



Combined events:

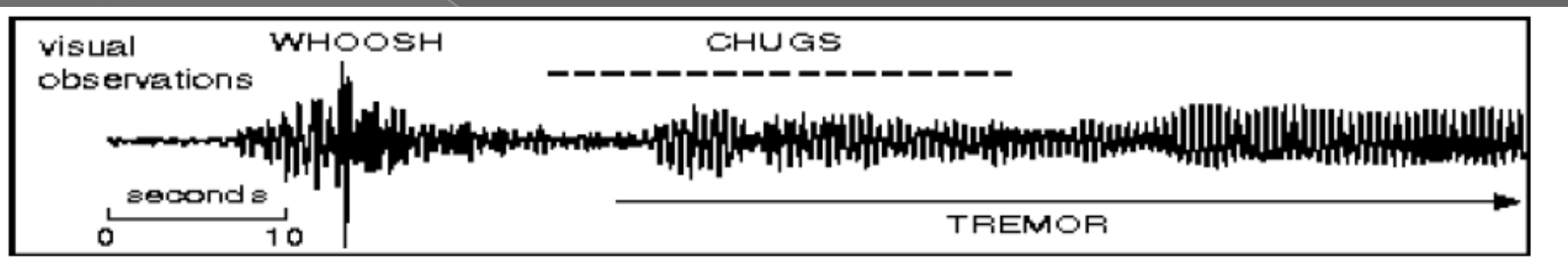
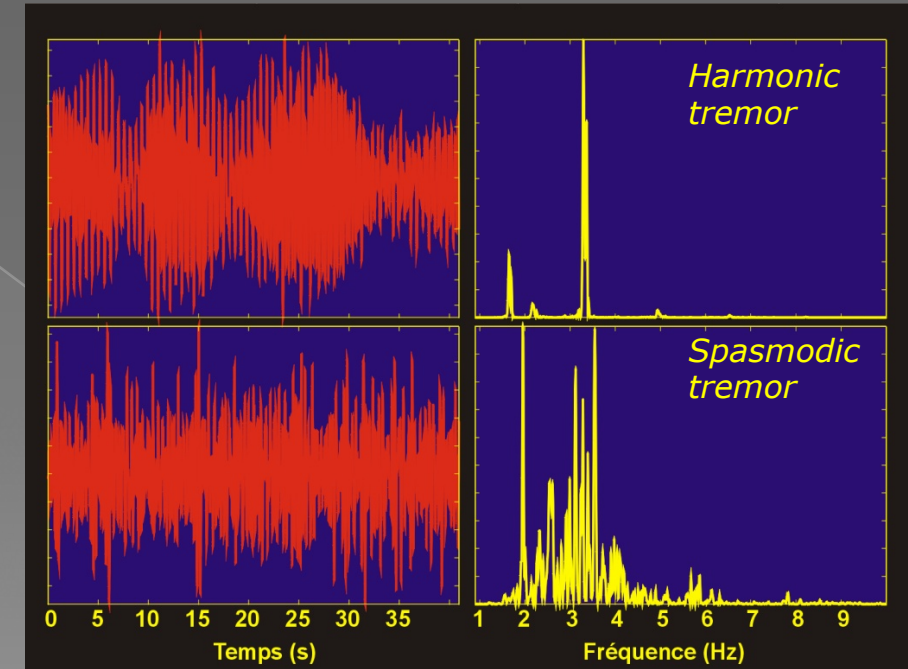
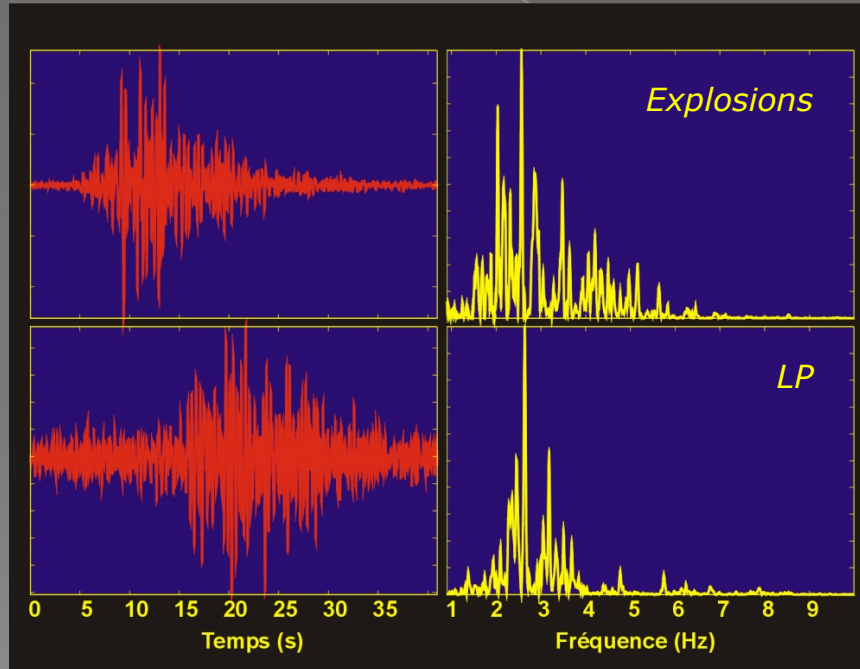


Figure 2. An example seismogram (radial component) of a small eruption (whoosh) followed by rhythmic degassing (chugs). Visual and audio observations show this eruption ejecting ash to ~500 m above the crater and the following chugs were audible at 2.8 km for ~25 s. Harmonic tremor begins during the chugs and continues for several minutes.

Benoit & McNutt (1997)

2. Classification of seismic signals:

Four basic type of events:



3. Characterization of seismic events:

Discrete Fourier analysis:

Hagerty et al. (2000)

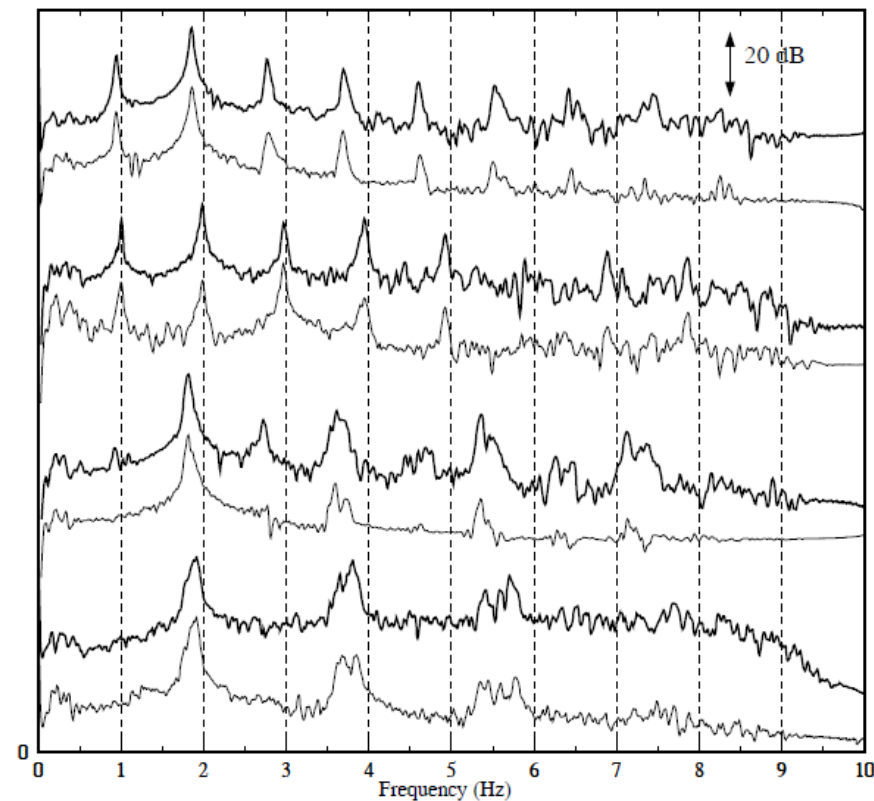


Fig. 18. Normalized log spectral density plots for four isolated, non-continuous 30 s tremor slices recorded at WARN (thick line) and LOLA (thin line). The spectra for different time slices vary considerably but are nearly identical at the two stations.

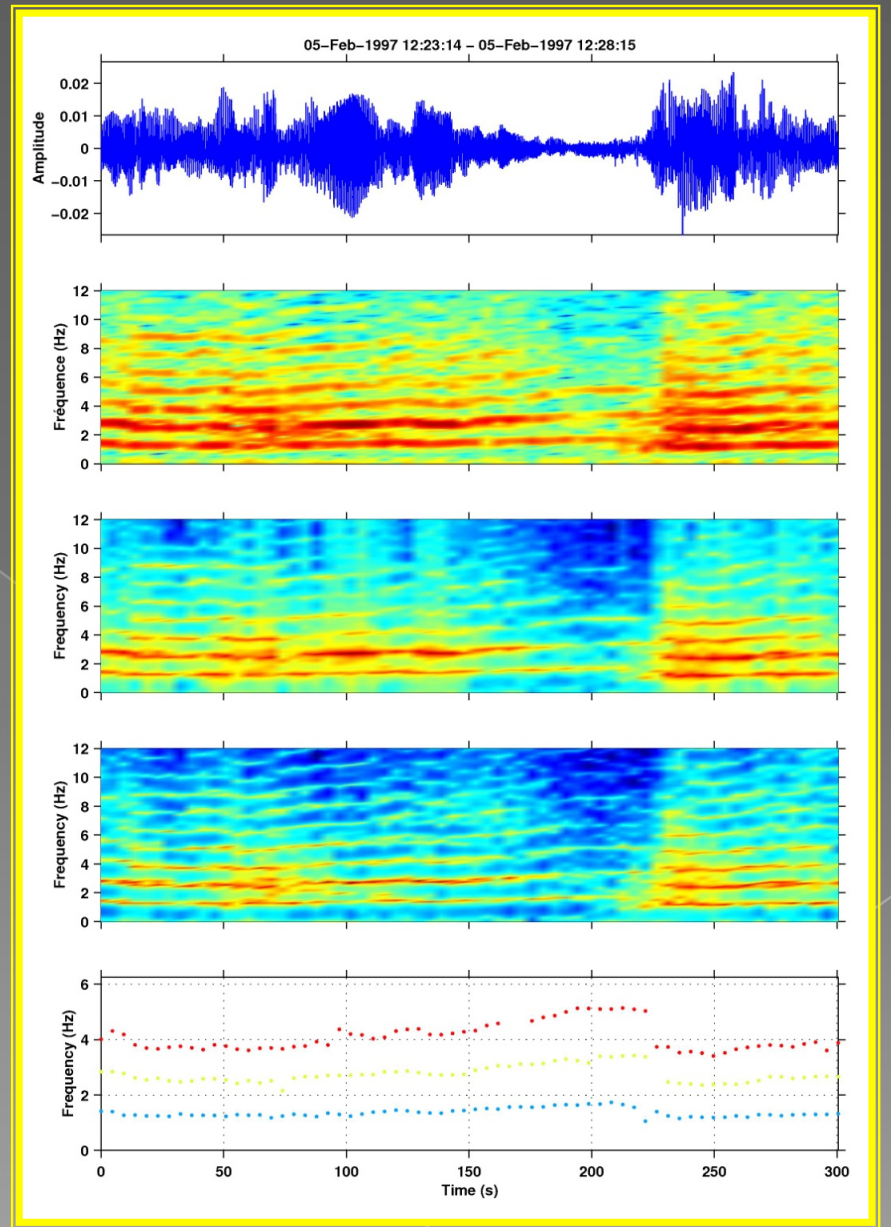
Time-frequency analysis:

Fourier spectra

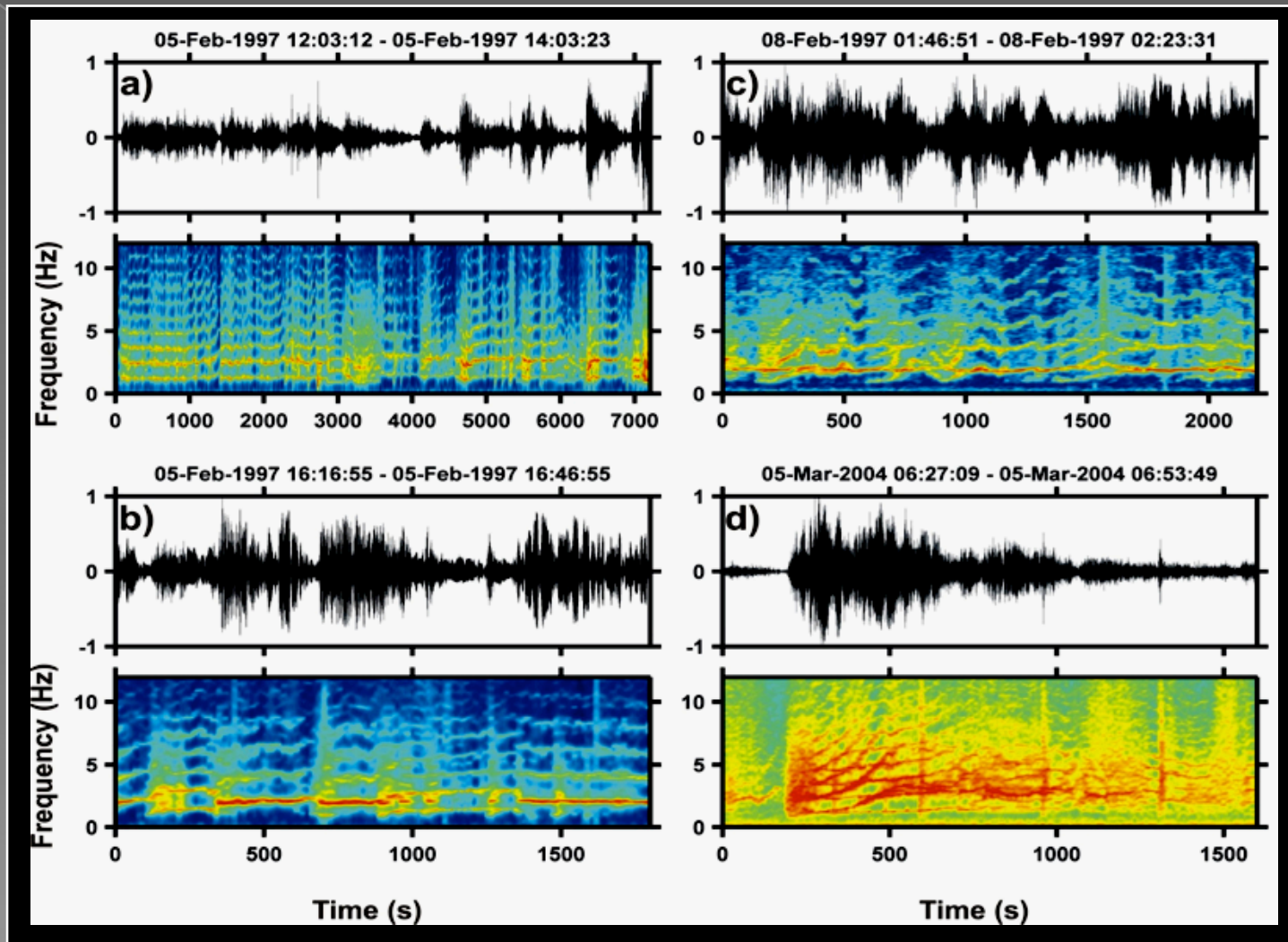
AR filters
(Yule – Walker algorithm)

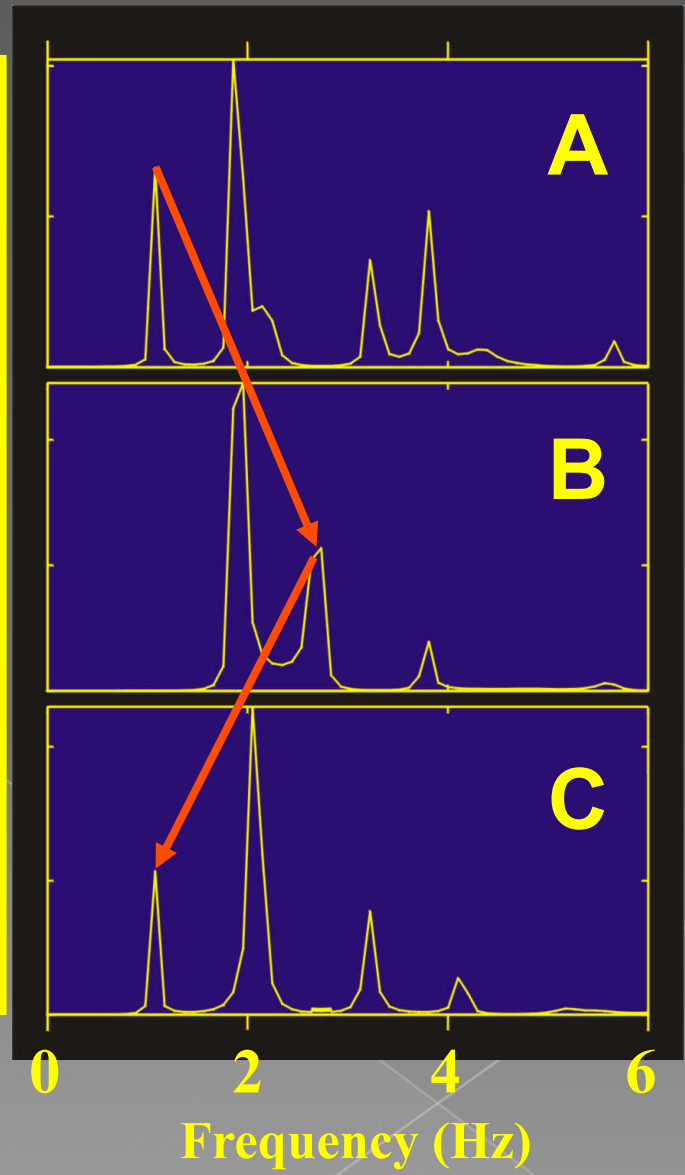
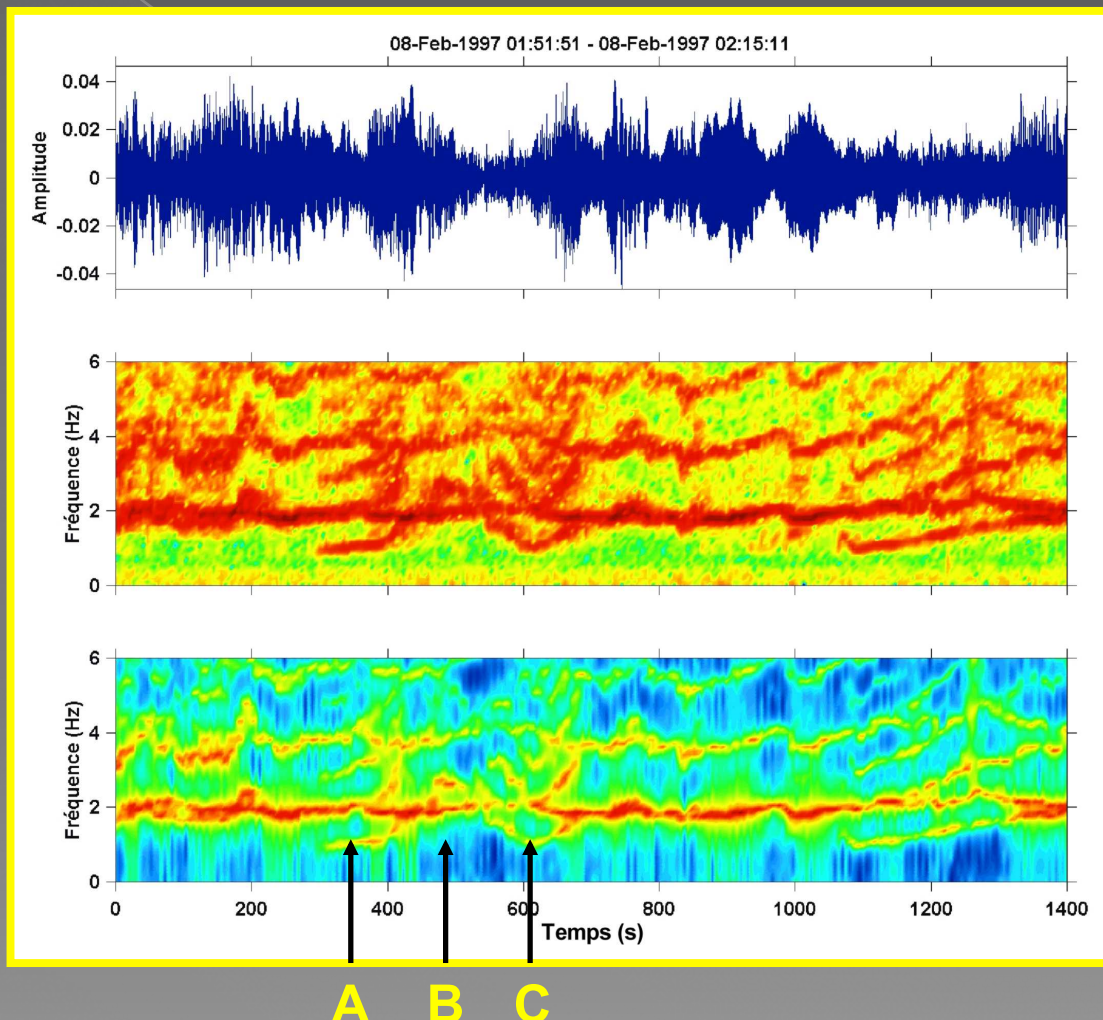
Burg method

AR poles representation

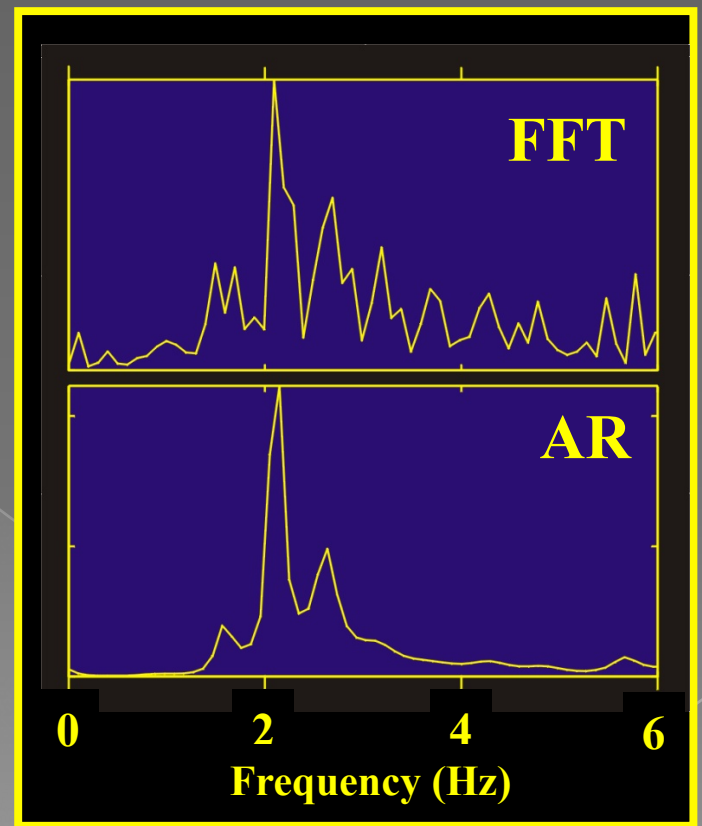
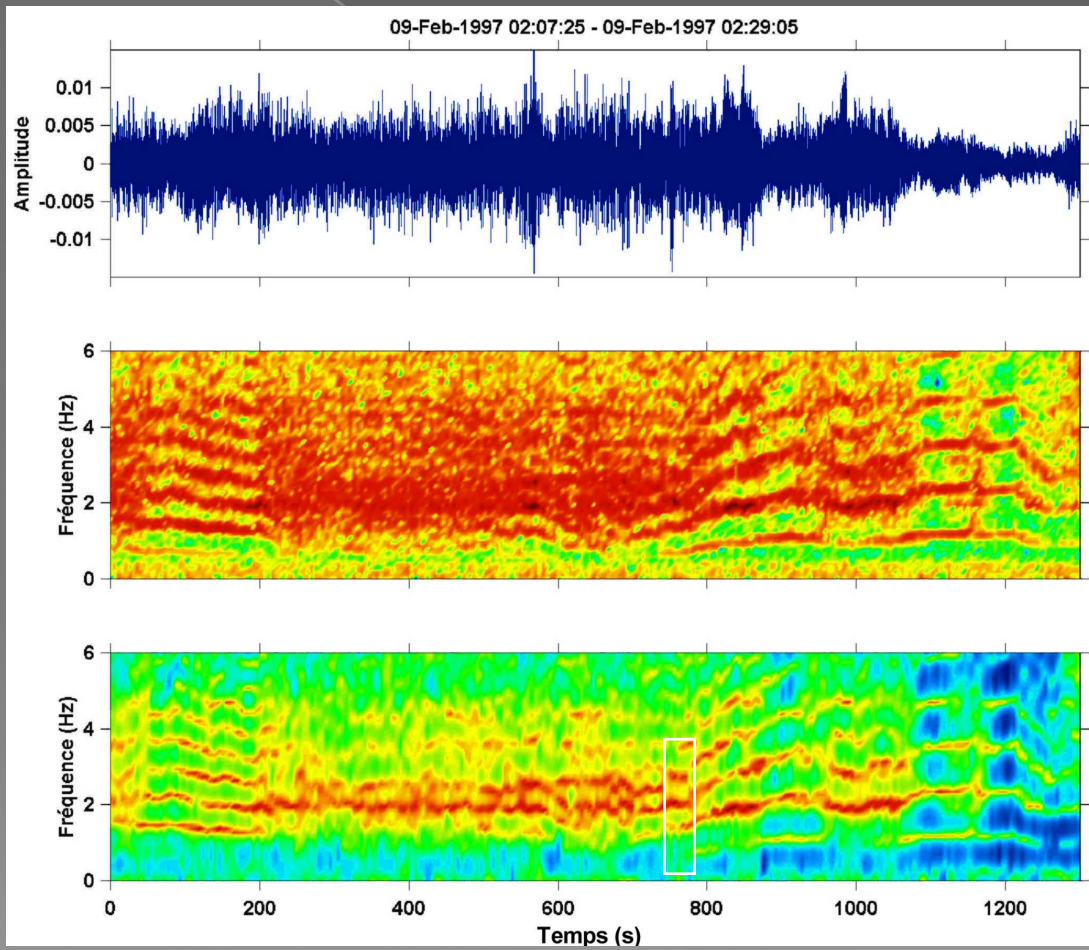


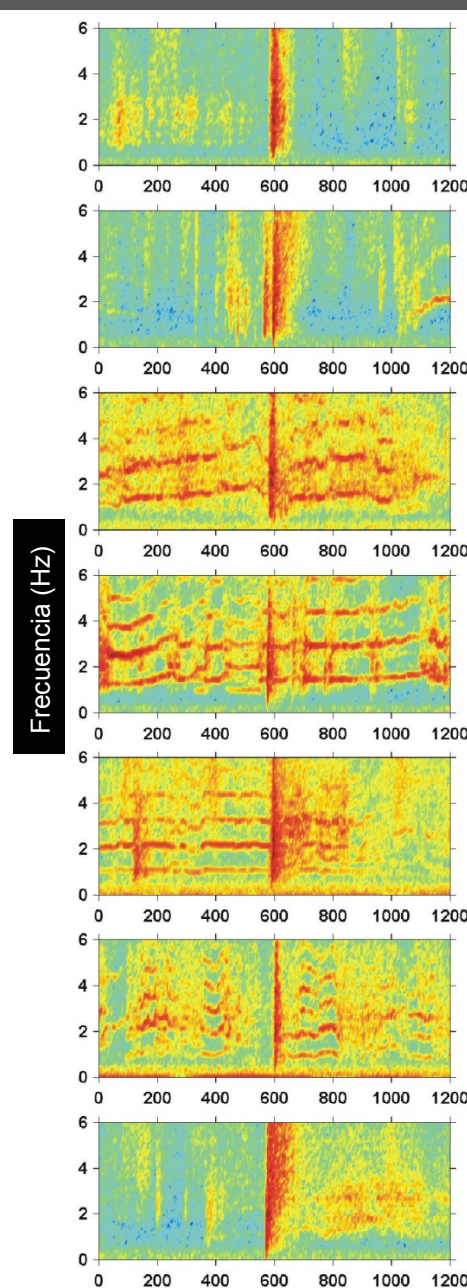
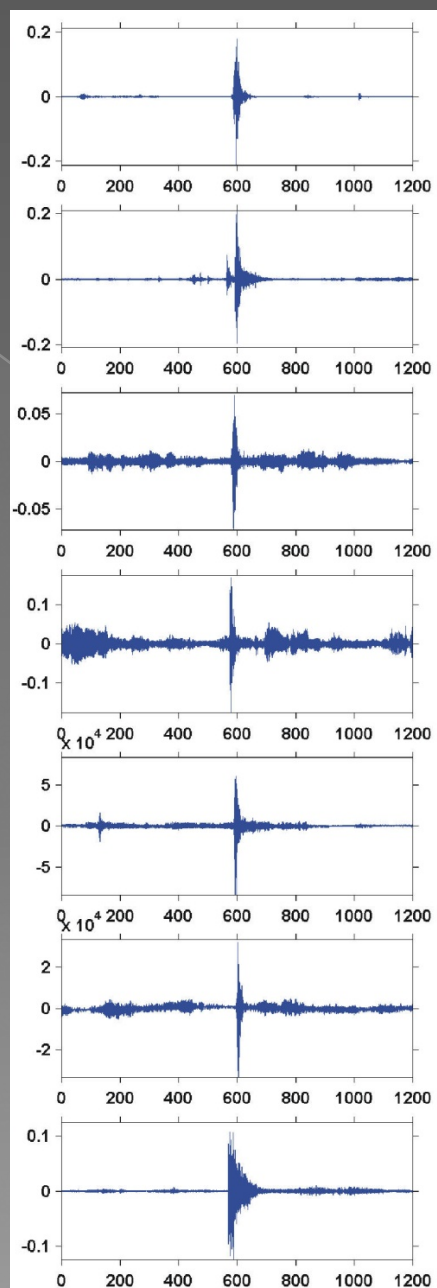
Complex behavior of volcanic tremors and superposition of events (Lesage et al, 2006)

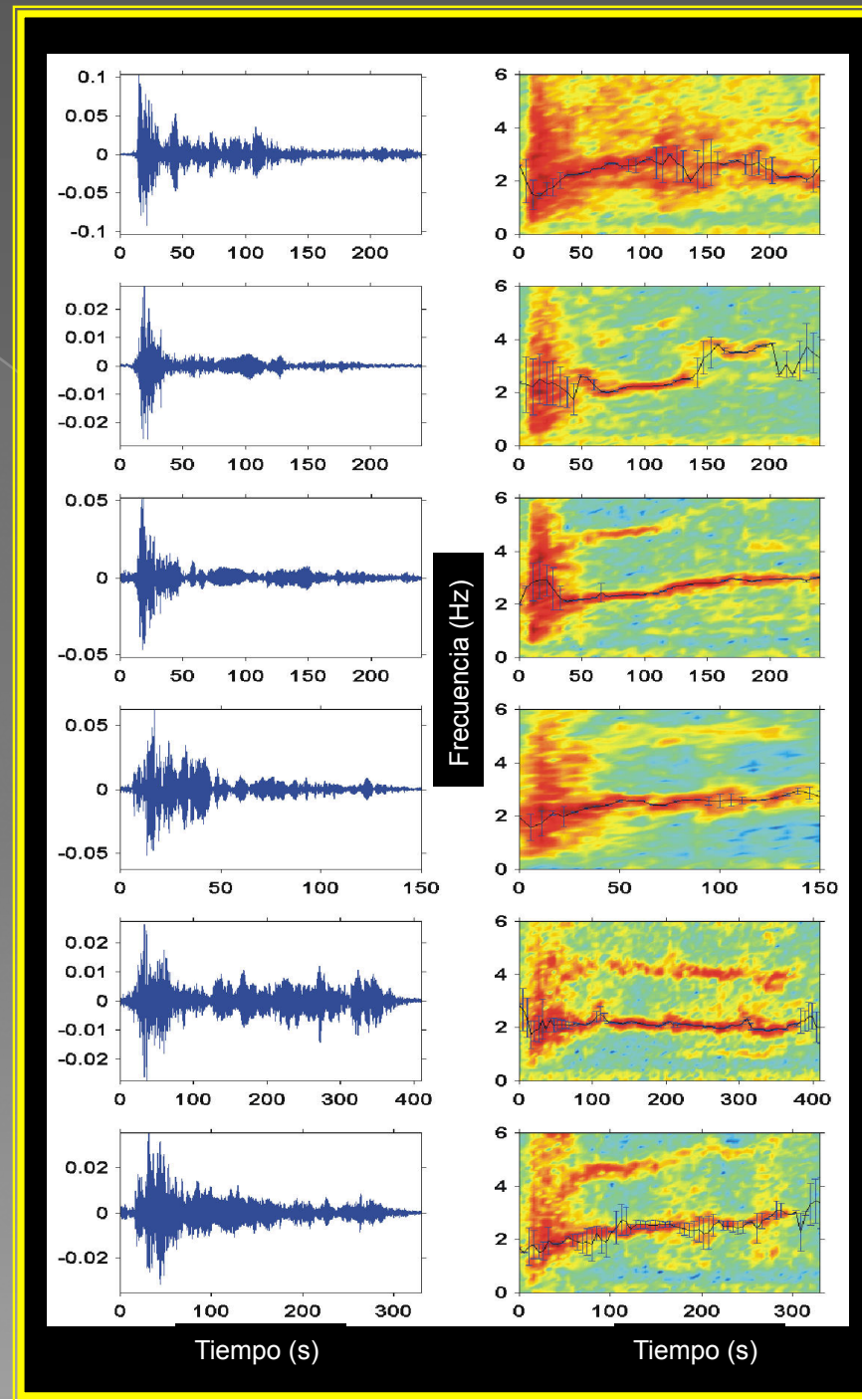


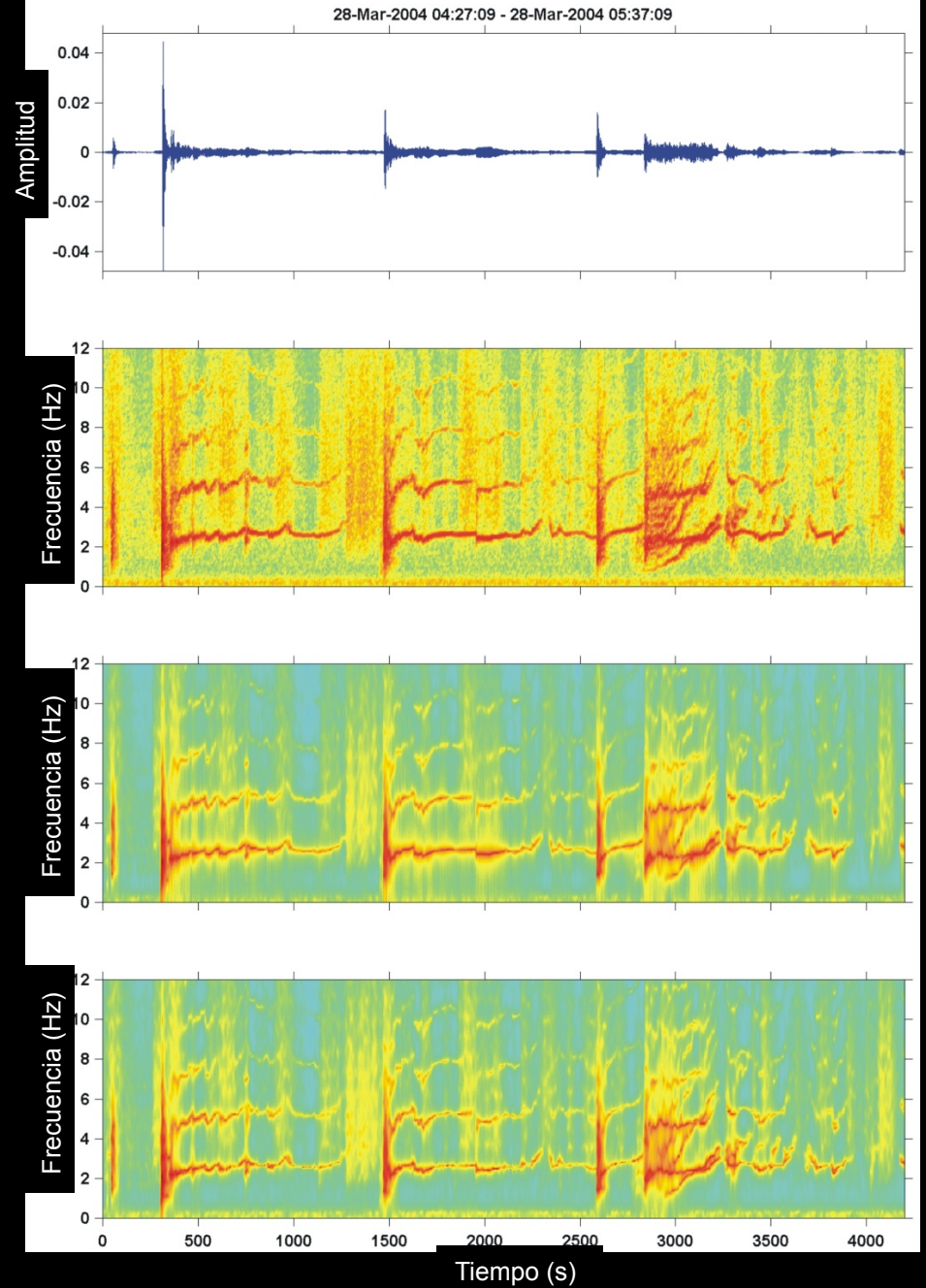


Spasmodic tremor of Arenal volcano, Costa Rica (Lesage et al,2006)









5. Study of seismic site effects:

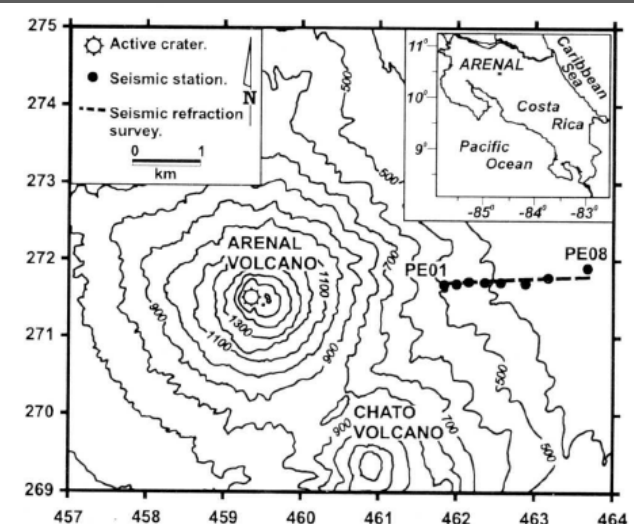


Figure 1. Arenal volcano, Costa Rica. Location of the east linear array used in this study and the seismic refraction survey, which provided the shallow velocity structure.

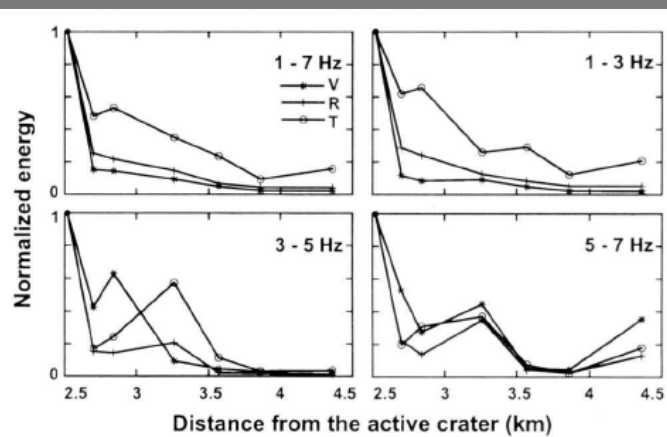


Figure 3. Tremor energy as a function of the distance from the active crater along the radial array, in several frequency bands. All the calculated energies are normalized by the corresponding values at station PE01. V: vertical, R: radial, T: transverse component.

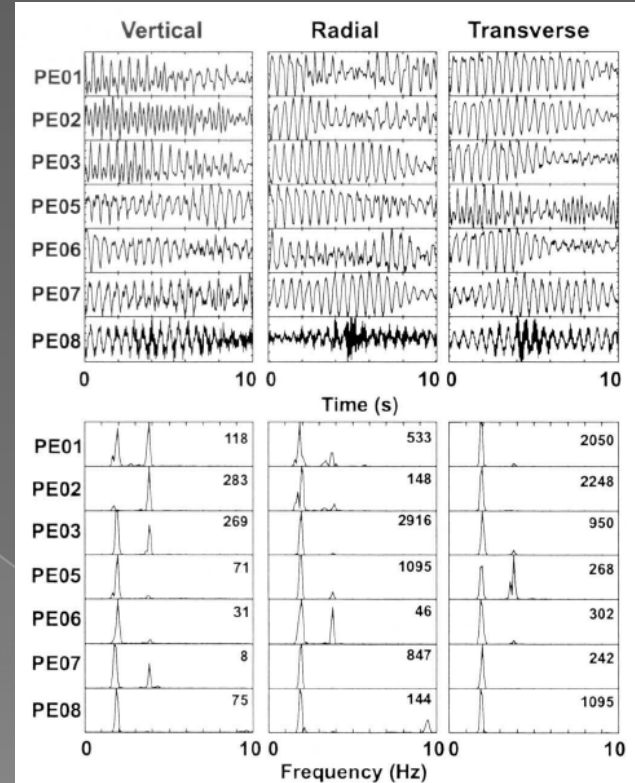
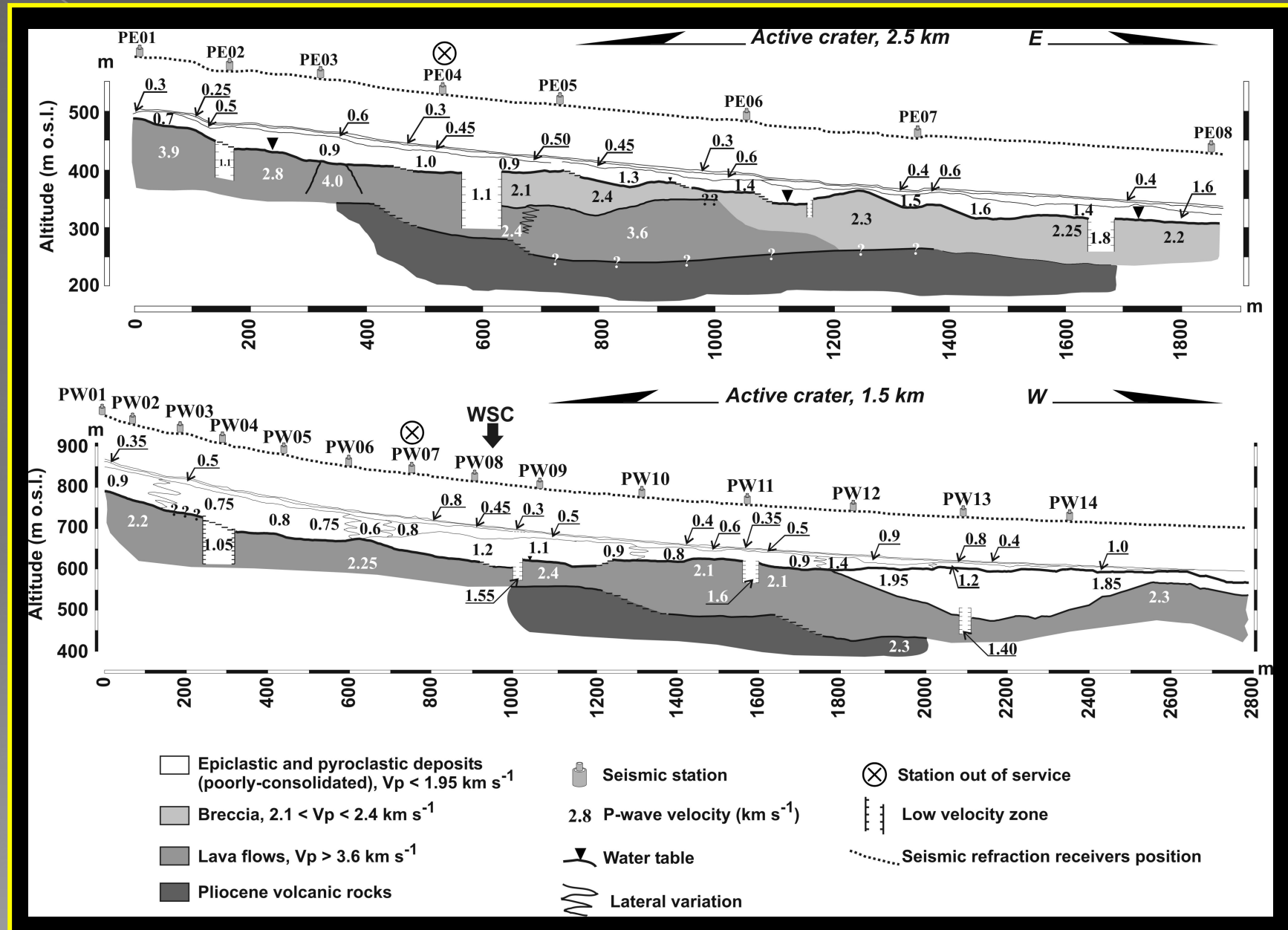


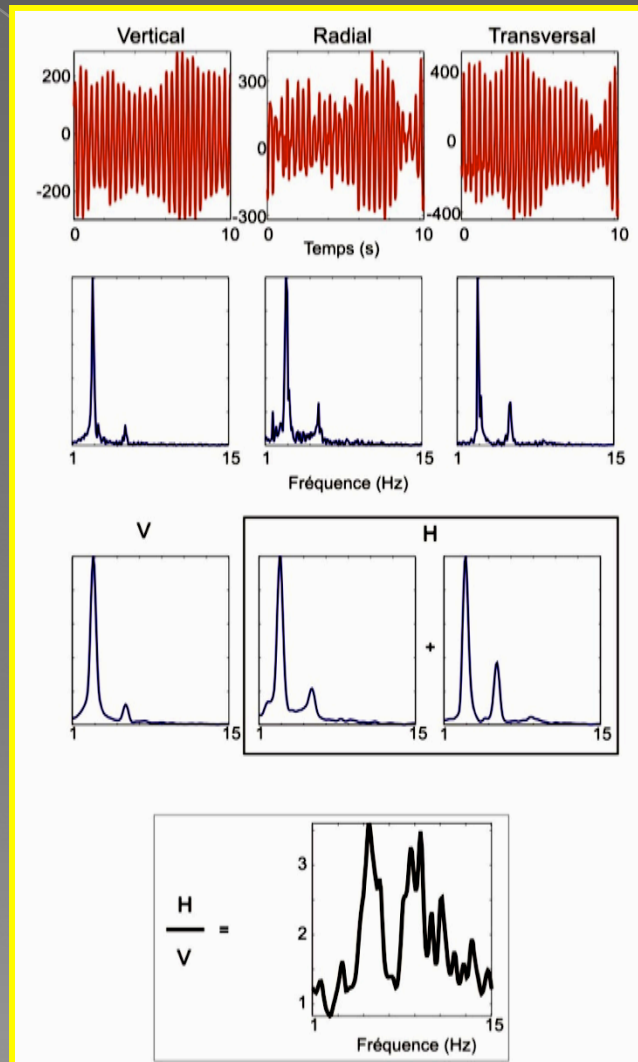
Figure 2. Three components waveforms (top) and corresponding normalized power density spectra (bottom) of a harmonic tremor section recorded along the east linear array. Numbers at the upper right corner of the spectra corresponds to the maximum amplitude. No records are available at station PE04 because of a recorder failure.

Seismic refraction models



H/V spectral ratios (Nakamura, 1989)

Signal
FFT
Smoothed
FFT
Spectral
ratio



H component:

$$H(f) = \sqrt{\frac{|U_{sr}^2(f)| + |U_{st}^2(f)|}{2}}$$

U_{sr} = radial component.

U_{st} = transverse component.

Average (Field & Jacob, 1995):

$$\ln \bar{Z} = \frac{1}{N} \sum_{n=1}^N \ln \left(\frac{H_n}{V_{sn}} \right) = \frac{1}{J} \sum_{n=1}^N (\ln H_n - \ln V_{sn})$$

$$\sigma_{std} = \left\{ \frac{1}{N-1} \sum_{n=1}^N [(\ln H_n - \ln V_{sn}) - \ln \bar{Z}]^2 \right\}^{\frac{1}{2}}$$

N = number of windows.

H_n y V_{sn} = smoothed spectra.

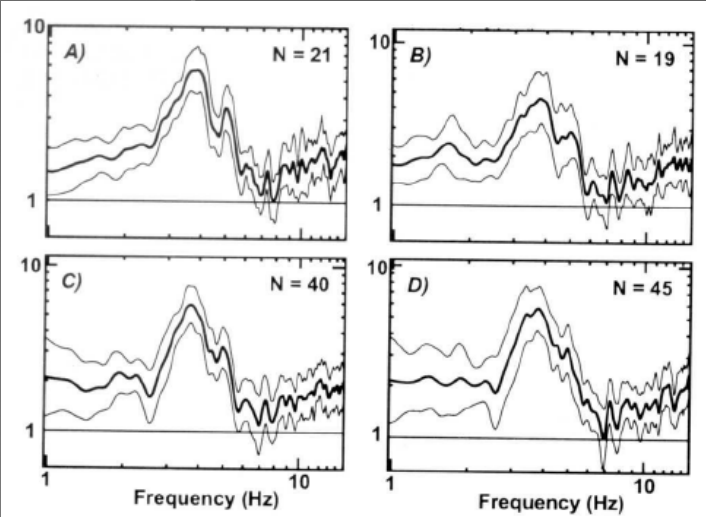


Figure 4. Mean H/V spectral ratios (solid lines) and mean ratios ± 1 standard deviation (thin lines) at station PE05, calculated by using different types of signal : a) seismic noise, b) long-period events and explosions, c) spasmodic tremor, d) harmonic tremor. N in the upper right corner is the number of signal sections used for computing the average and the standard deviation.

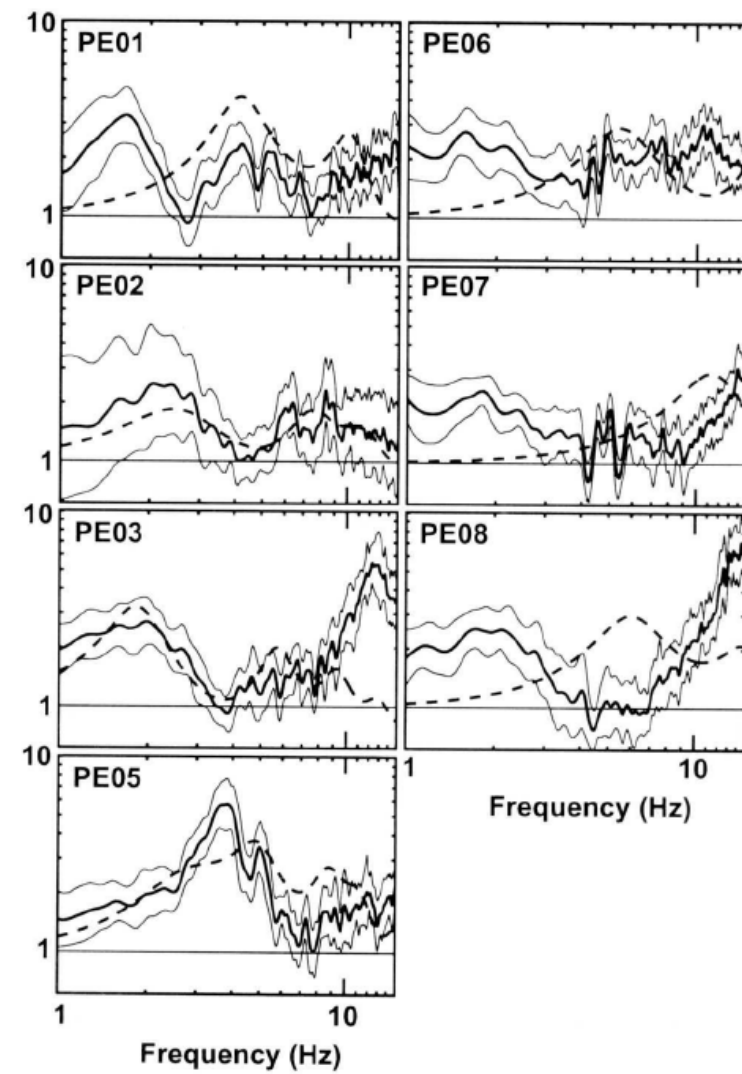
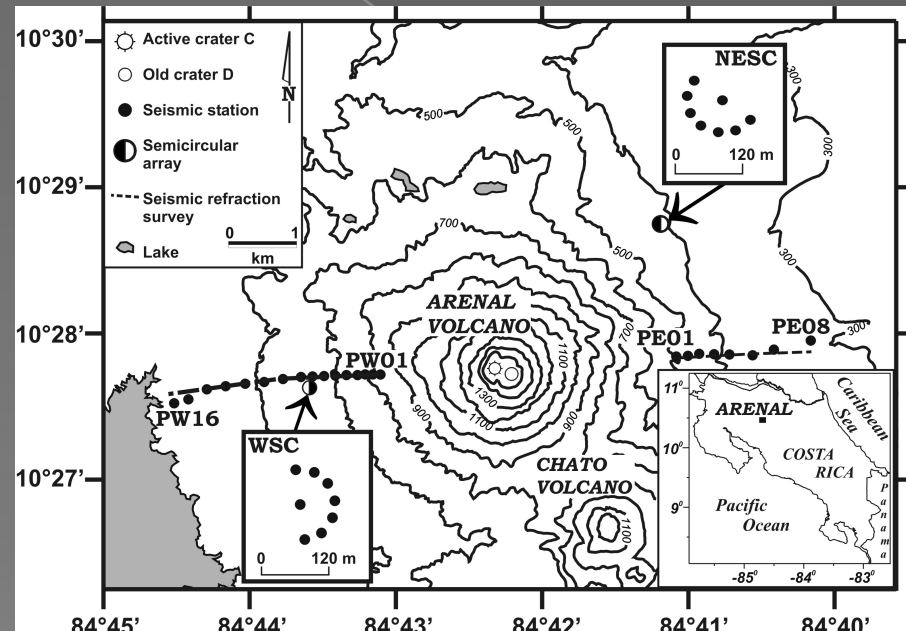


Figure 5. Mean H/V ratios (solid lines), calculated with 21 slices of ambient noise, mean ratios ± 1 standard deviation (thin lines) and theoretical S-wave transfer functions (dashed lines) for the stations of the linear array.

5. Study of structure:



Spatial correlation method (Aki, 1957)

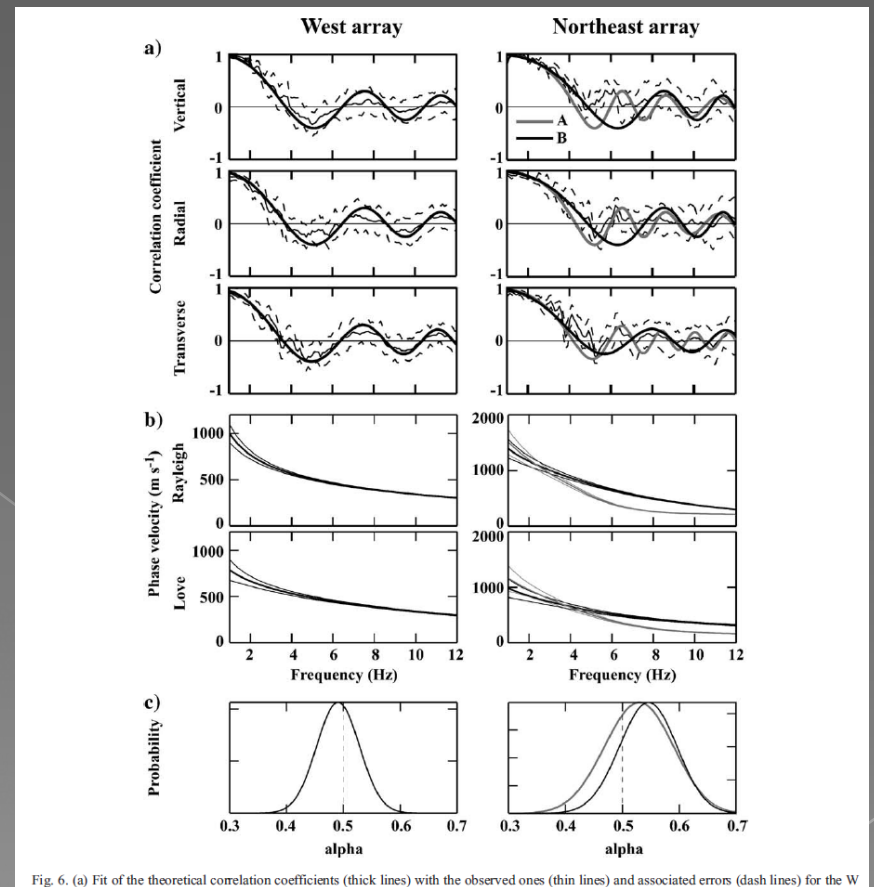
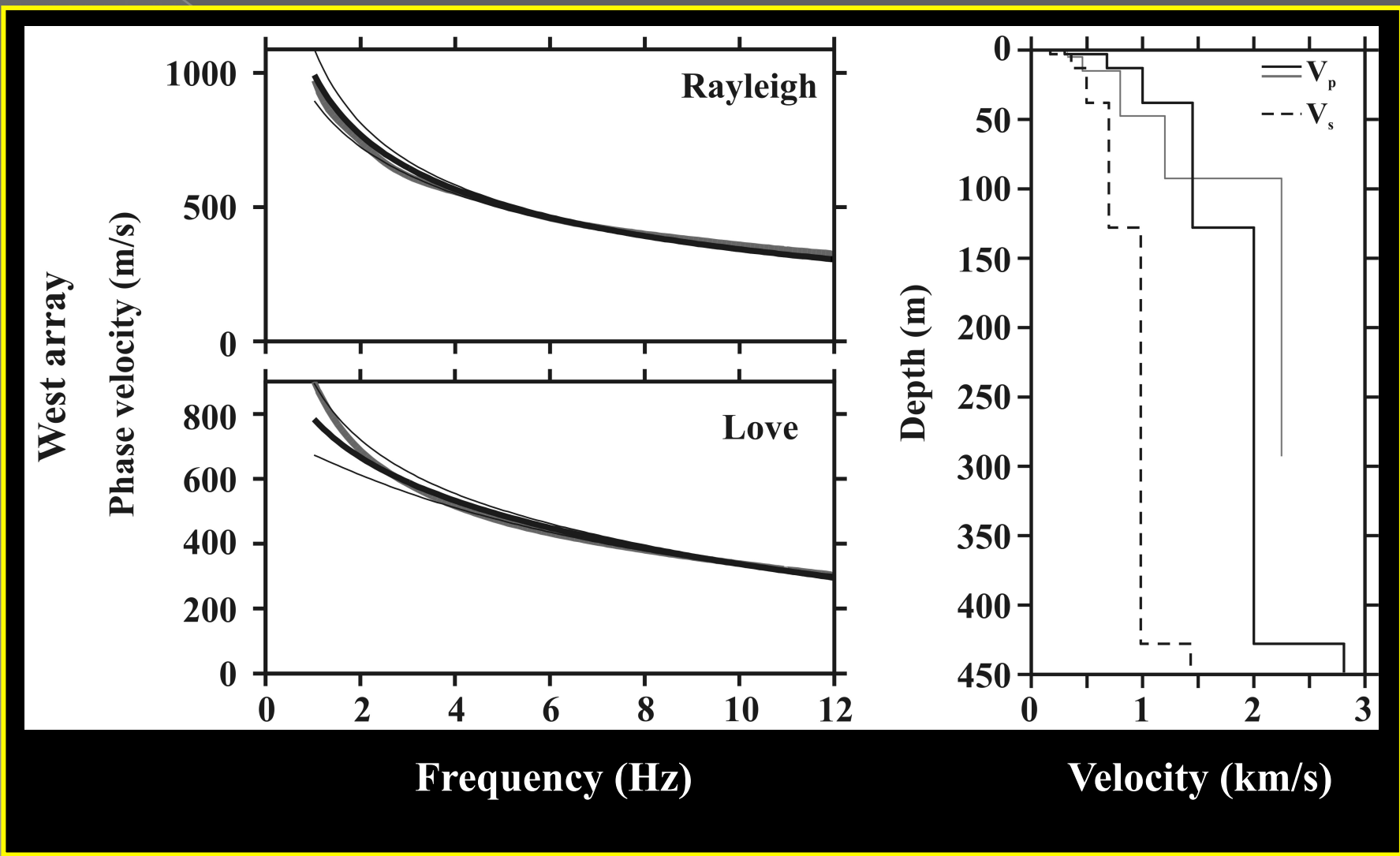


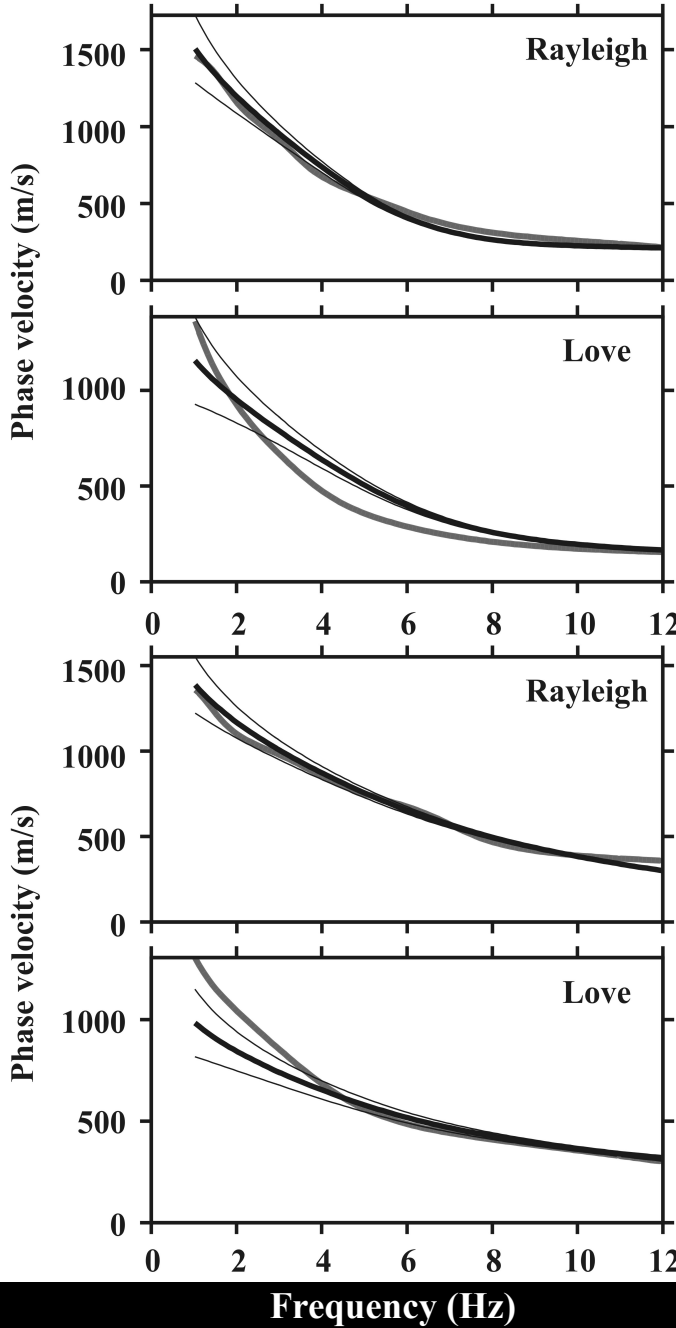
Fig. 6. (a) Fit of the theoretical correlation coefficients (thick lines) with the observed ones (thin lines) and associated errors (dash lines) for the W (left) and NE (right) arrays. (b) Estimated phase velocities (thick lines) of the Rayleigh and Love wave and corresponding errors (thin lines). (c) Probability functions associated to the proportion α of Rayleigh wave. The dash line ($\alpha=0.5$) represents equal proportions of Rayleigh and Love waves. For the NE array, the two solutions obtained in the inverse problem, A (gray) and B (black), are shown.

Velocity model: West array

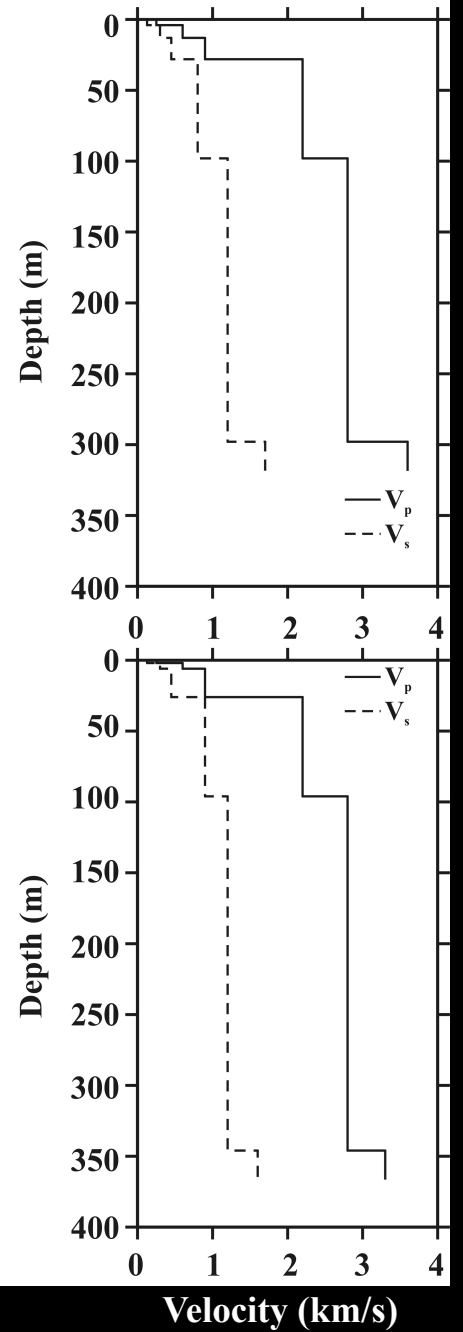
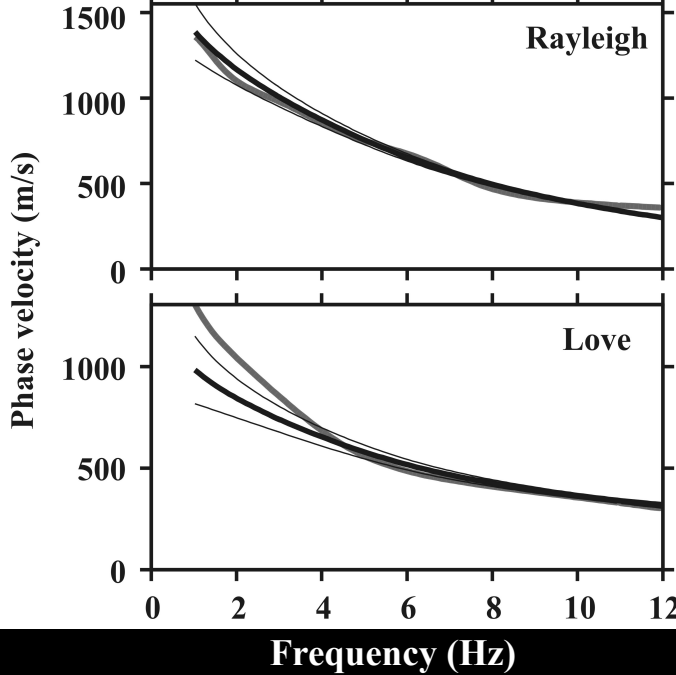


Velocity models: Northeast array

Northeast array (Solution A)

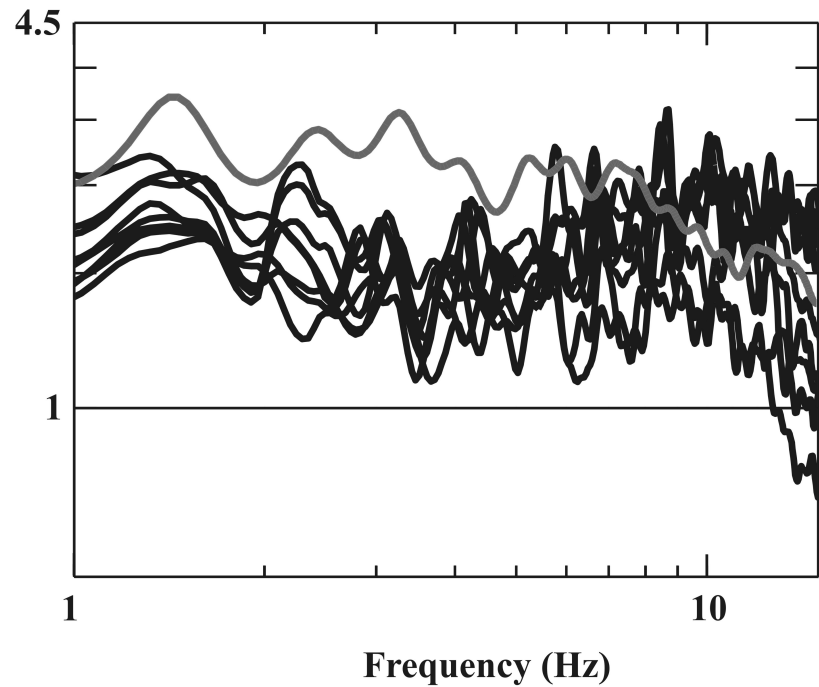


Northeast array (Solution B)

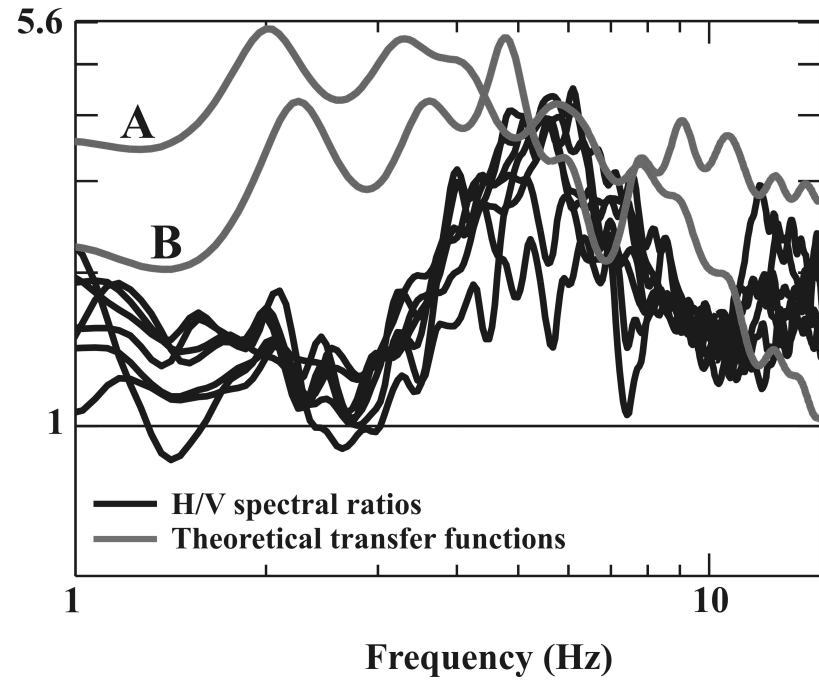


Spectral ratios

West array

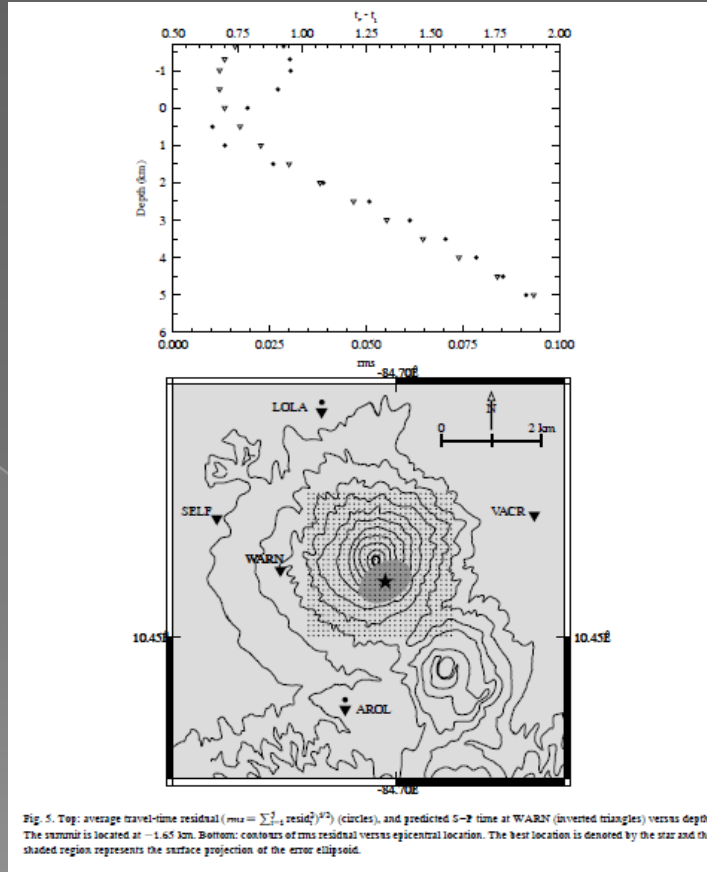
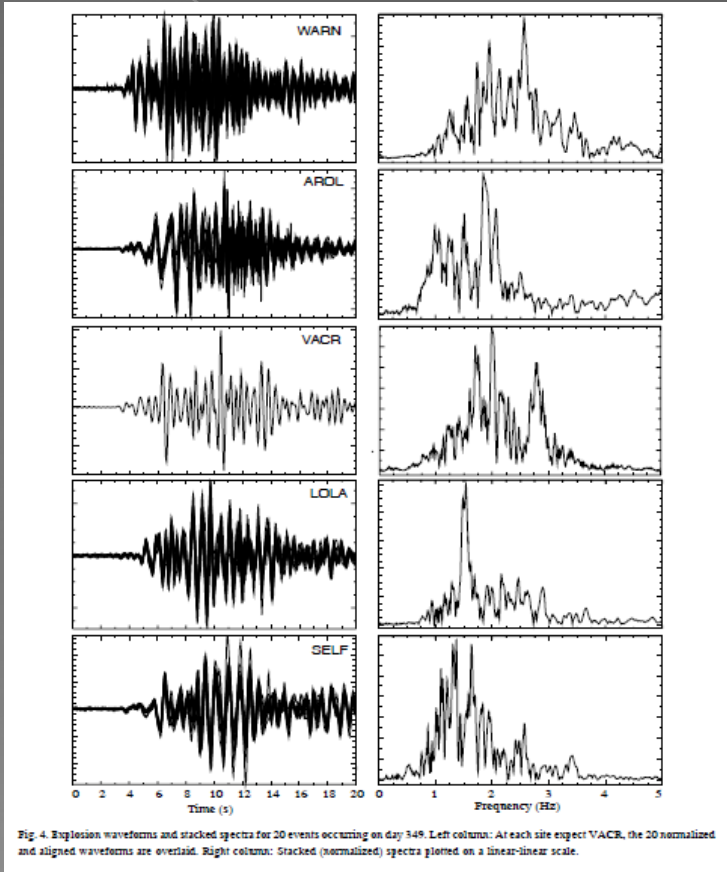


Northeast array



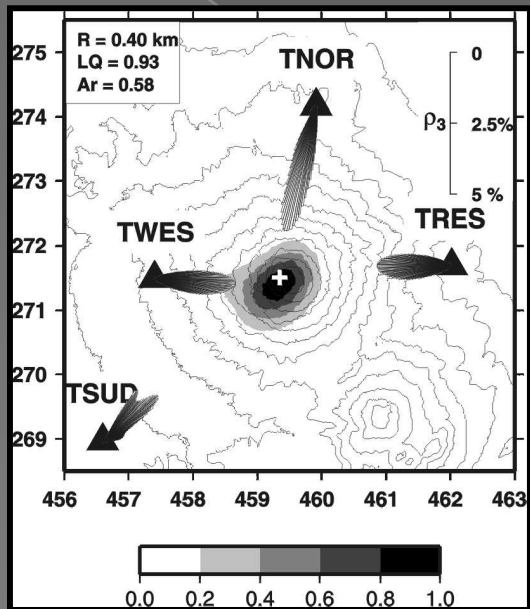
— H/V spectral ratios
— Theoretical transfer functions

6. Source event location:



Hagerty et al. (2000)

2 mn of tremor

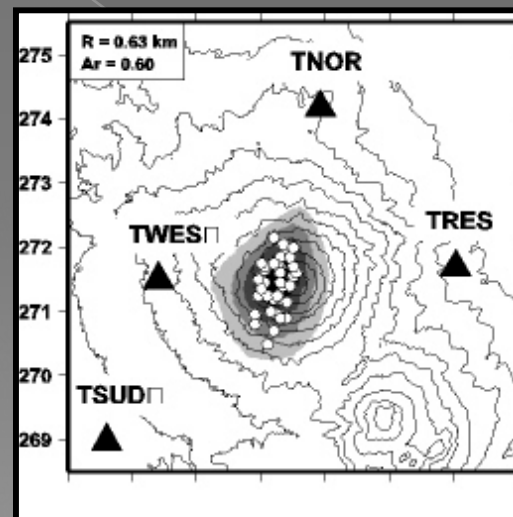


4 triangular arrays + 1 "L"

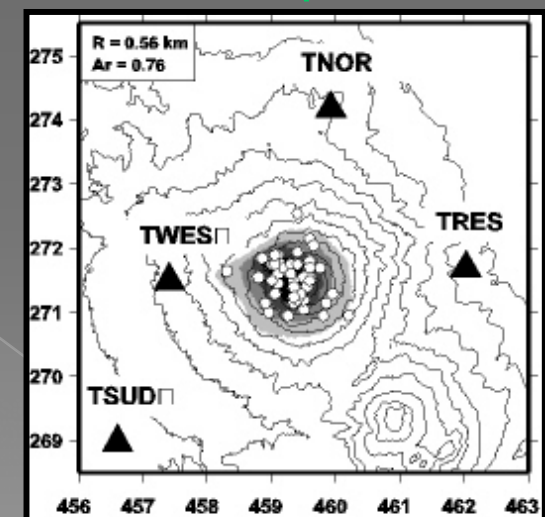
accuracy:

- > tremor : $\sim 600 \text{ m}$
- > explosions : $\sim 450 \text{ m}$

45 tremors



50 explosions



Seismic zone:

- 600 m radius
- over the crater

Métaxian et al. (2002)

8. Doppler radar and seismic experiments:

Valade et al. (in progress)

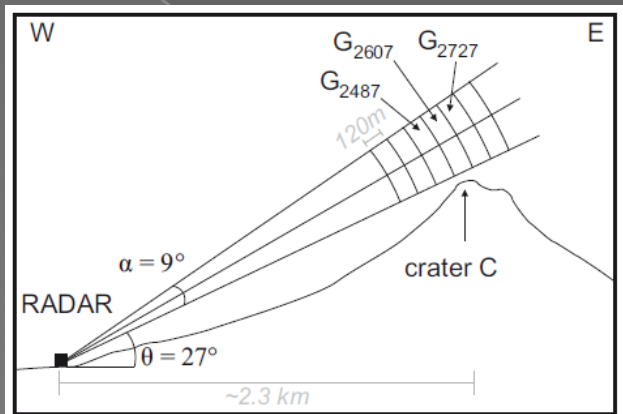
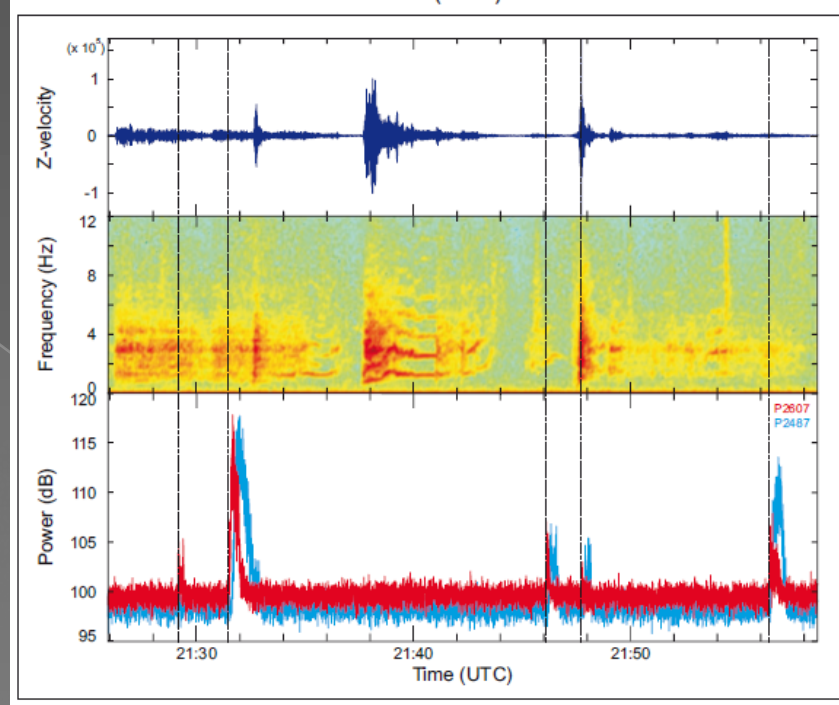


Figure 2. Radar sounding conditions during the recording campaign, between February 10 and 22, 2005.





Valade et al. (in prep.)

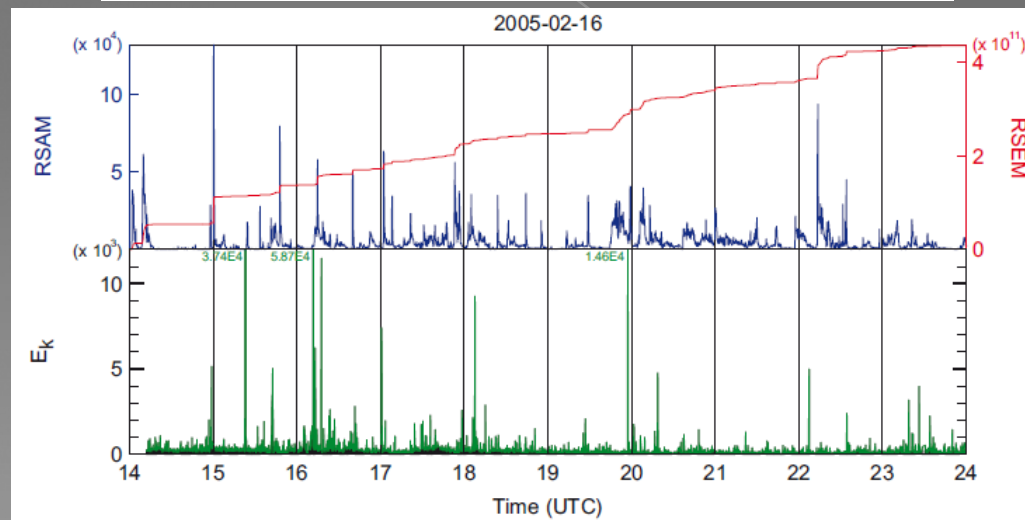


Figure 6. RSAM and RSEM (top) recorded on the 16th of February 2005, and E_k time series ($E_{k2607} + E_{k2727}$) (bottom). For visualization purposes the E_k ordinate axis was cut off at $E_k = 1.2E3$, the truncated peak values are consequently displayed. The green E_k curve is the envelope of the raw E_k curve. Computing parameters for RSAM and RSEM: window=10, threshold=3.

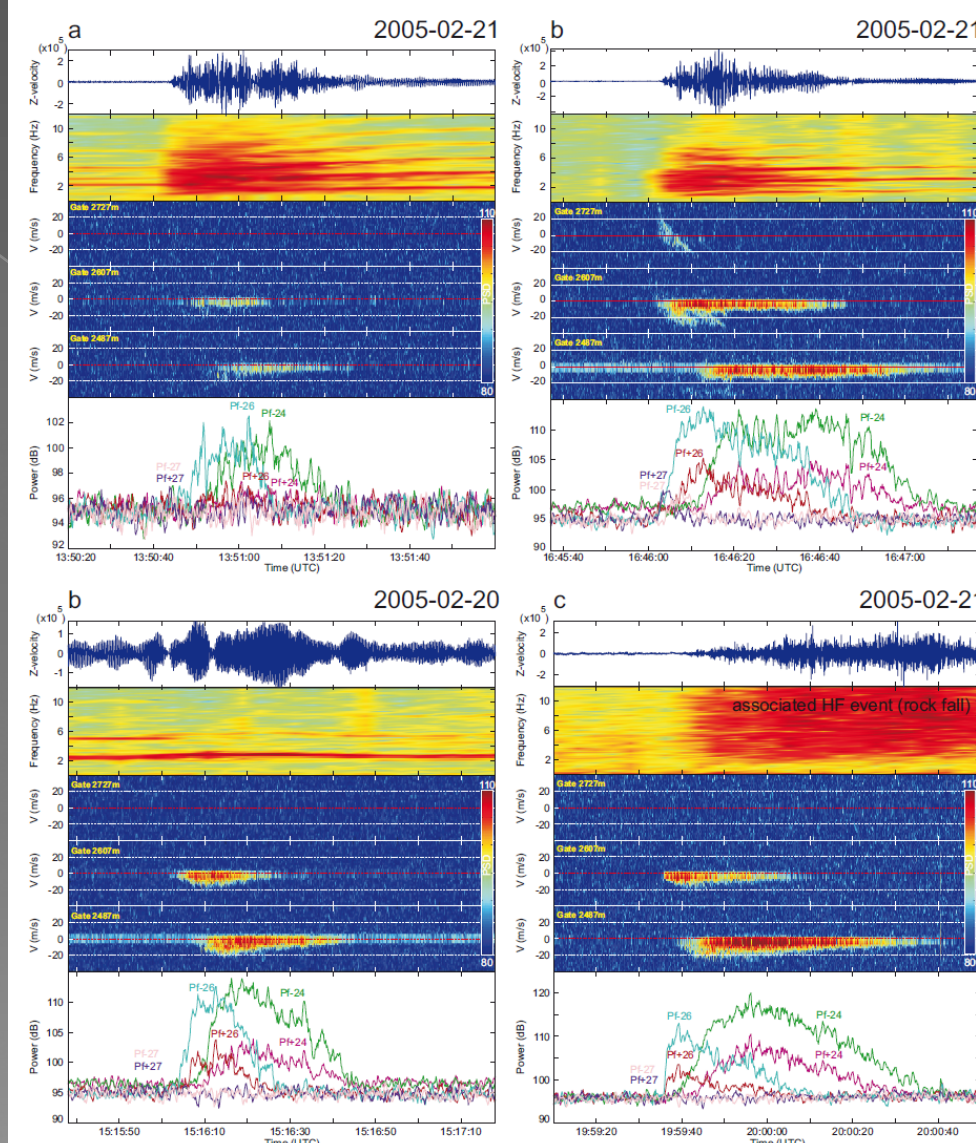


Figure 4. Diversity in both the seismic events associated to pyroclastic emissions (with (a) explosion type events, (b) during aseismic interval, and (c) during tremor sequence), and in the dynamics of these pyroclastic emissions. From top to bottom: seismic trace, seismic spectrogram, radargrams (Doppler spectra ($PSD = f(V)$)) as the function of time) of gates G_{2727} , G_{2607} , G_{2487} , time series of the recorded power in gates G_{2727} , G_{2607} , and G_{2487} .

9. Acoustic and seismic applications

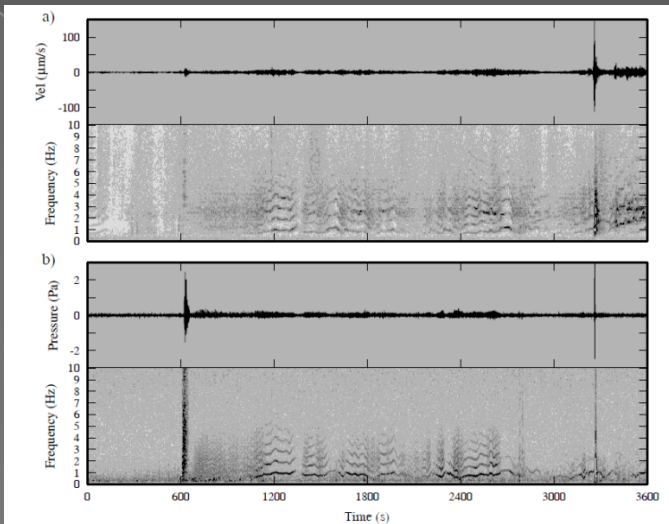


Fig. 21. (a) One hour of vertical velocity at WARN (top) and corresponding spectrogram (bottom). (b) Airborne acoustic pressure (top) and spectrogram (bottom) for the same period. Two summit explosions with different partitioning between the seismic and acoustic energy are separated by over 25 min of harmonic tremor that is clearly visible on both the seismic and acoustic channels.

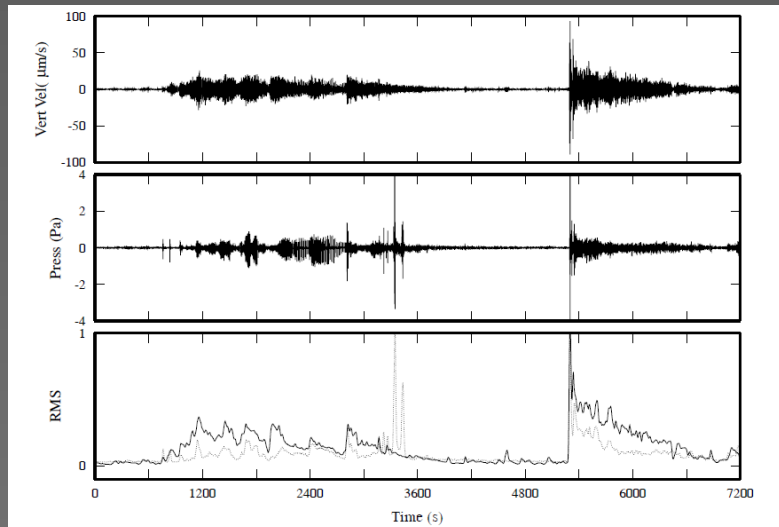


Fig. 22. Vertical velocity (top), acoustic pressure (middle), and RMS seismic (solid) and acoustic (dotted) energies (bottom) for the time period 117:03:30–05:30 recorded at WARN. Note the strong correlation between the acoustic and seismic RMS values, indicating good coupling between the seismic and acoustic wavefields.

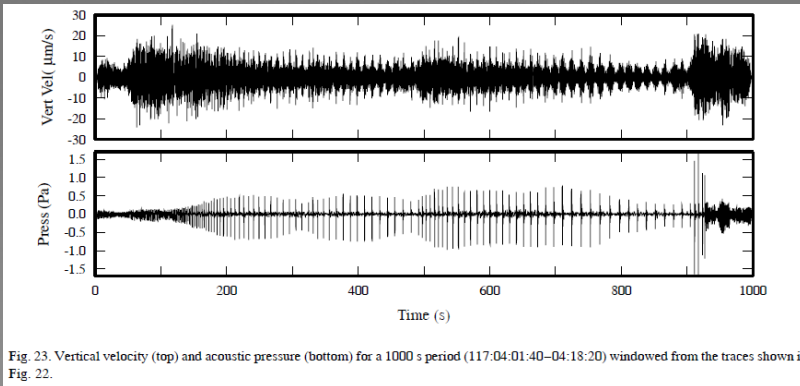


Fig. 23. Vertical velocity (top) and acoustic pressure (bottom) for a 1000 s period (117:04:01:40–04:18:20) windowed from the traces shown in Fig. 22.

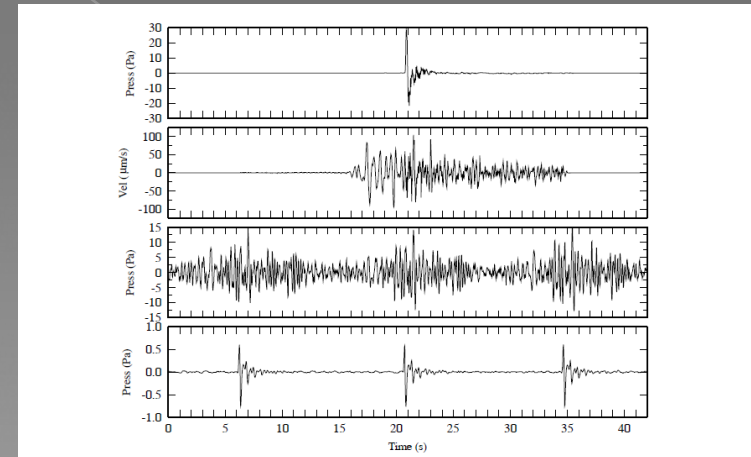
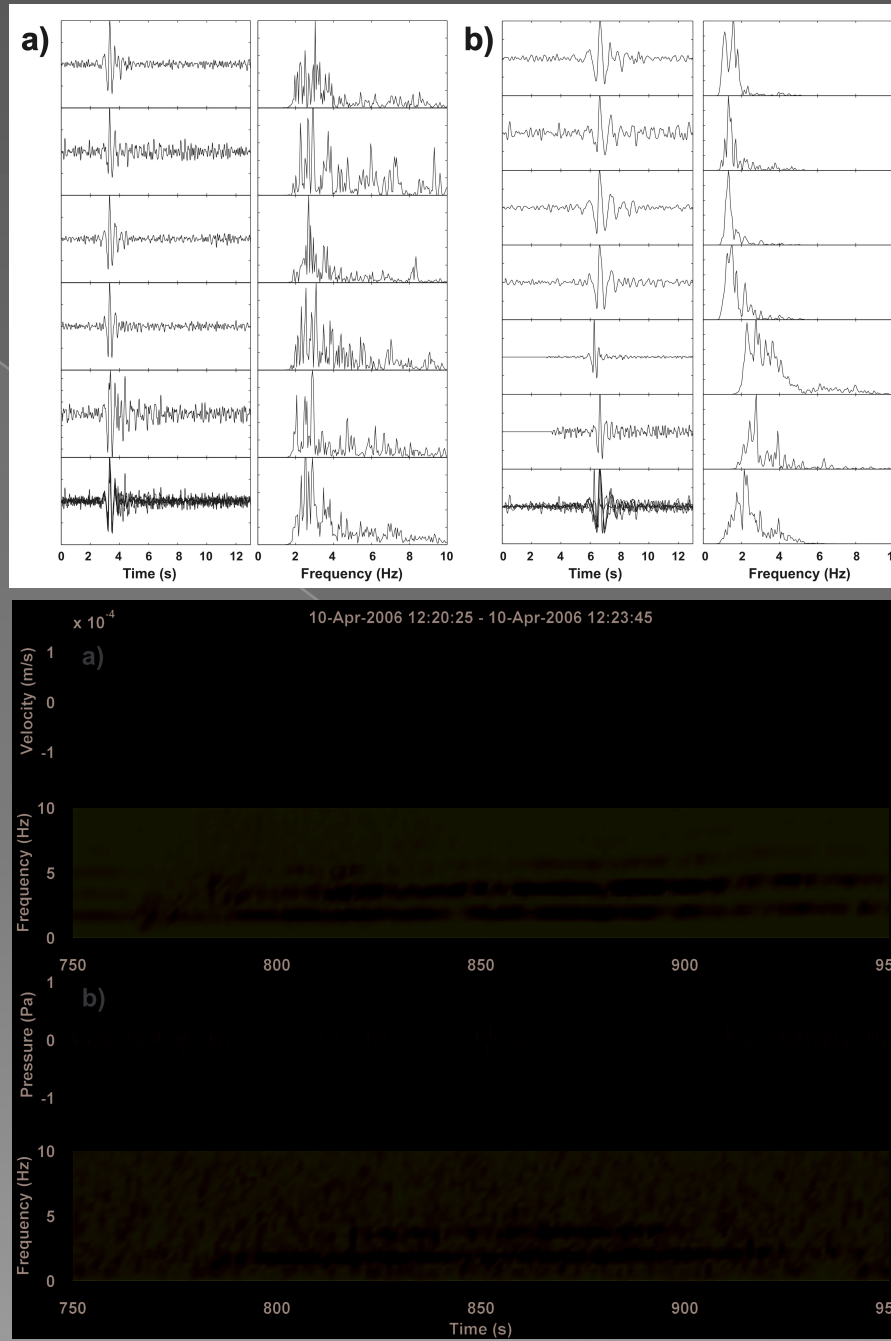


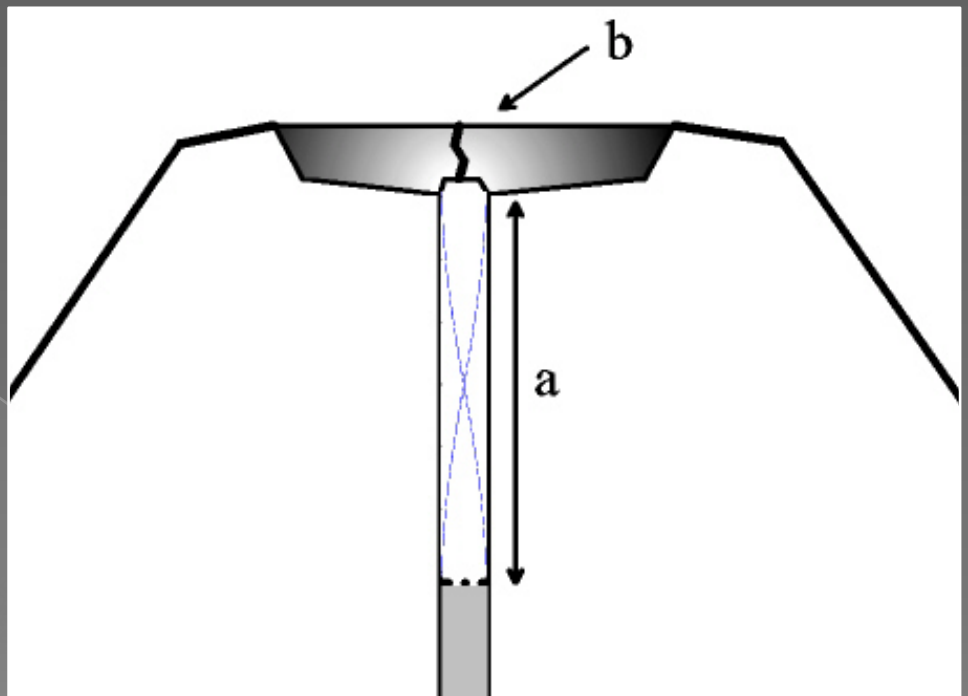
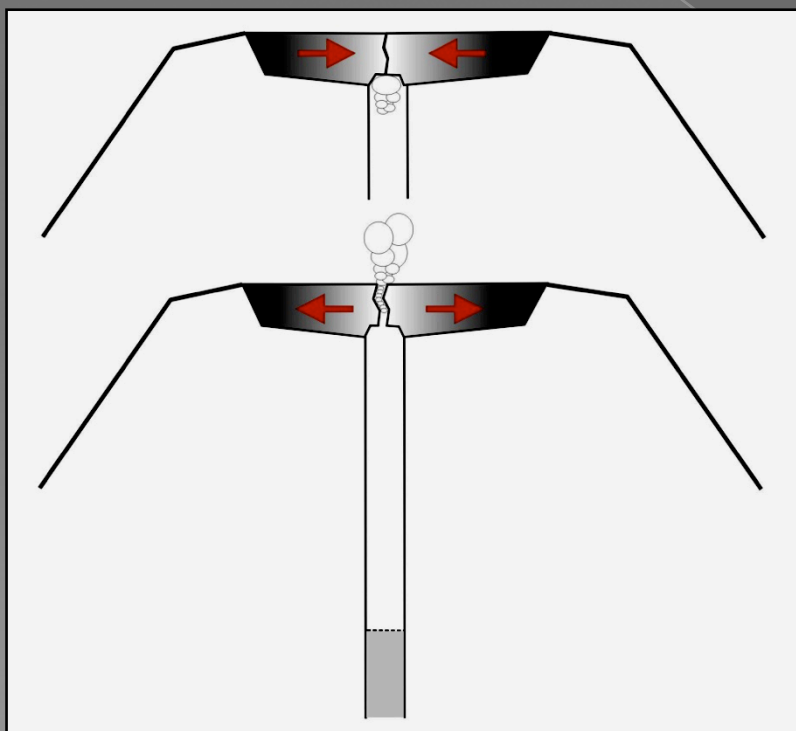
Fig. 24. Top: two traces: acoustic and seismic waveforms for the large summit explosion 122. Bottom two traces: acoustic and seismic waveforms for a zoomed in window taken from the explosion series shown in Fig. 23. Each seismic packet can be seen to correspond to an isolated explosion impulse in the acoustic channel.



Mora et al. (2009)

9. Conceptual modeling of tremor source:

Repetitive pulses stabilized by stationary waves on the tubes



a = Resonator conduit filled of magma + gas

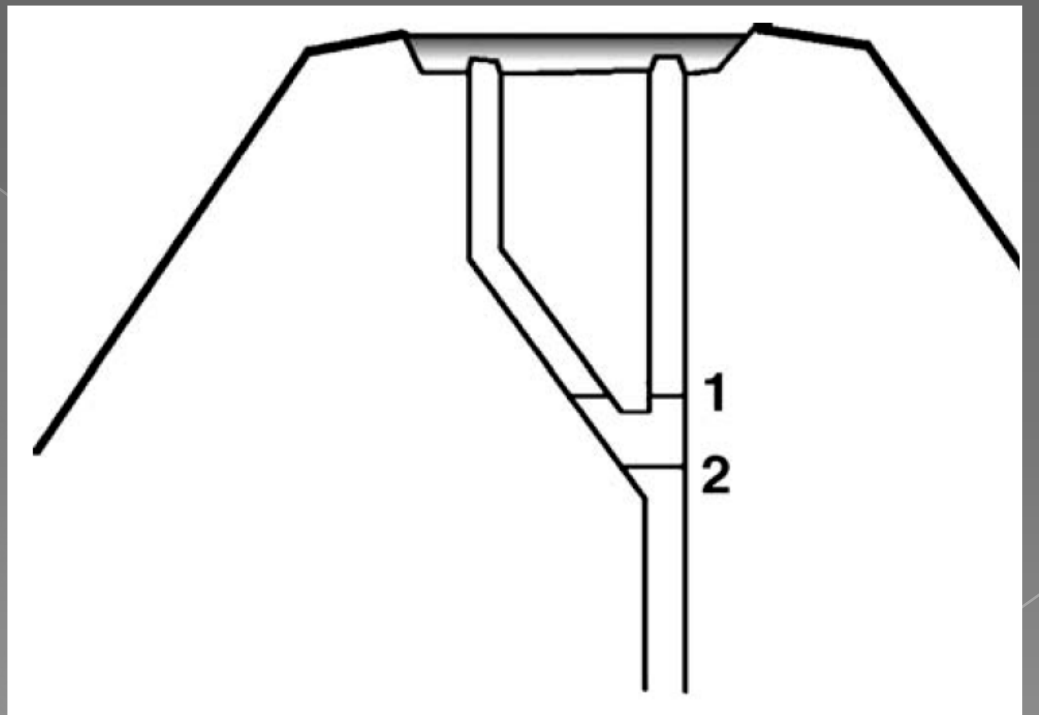
b = Lava plug.

Resonator limits = 1. plug, 2. bubble formation

Tremor double source

Nivel 1: 2 independent sources (high f_1)

Nivel 2: 2 connected sources
→ 1 resonator (low f_1)





Fotos de: L. Madrigal, 2004



Fotos tomadas de: www.arenal.net

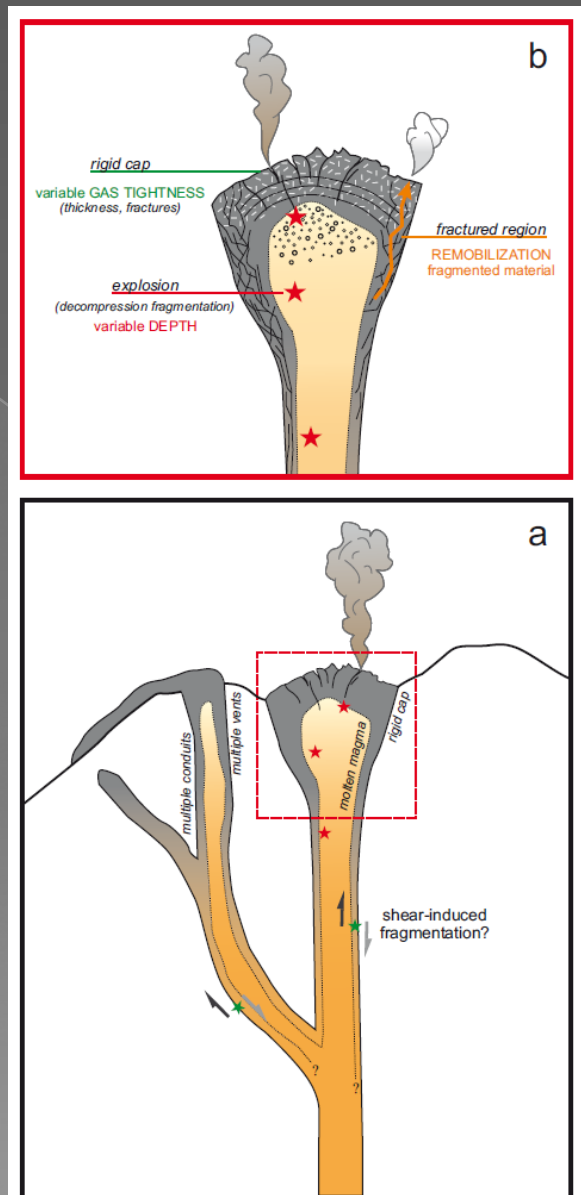


Figure 8. Conceptual model of Arenal's shallow structure, fragmentation mechanisms, and influencing parameters.

Valade et al. (in prep.)

TURRIALBA VOLCANO



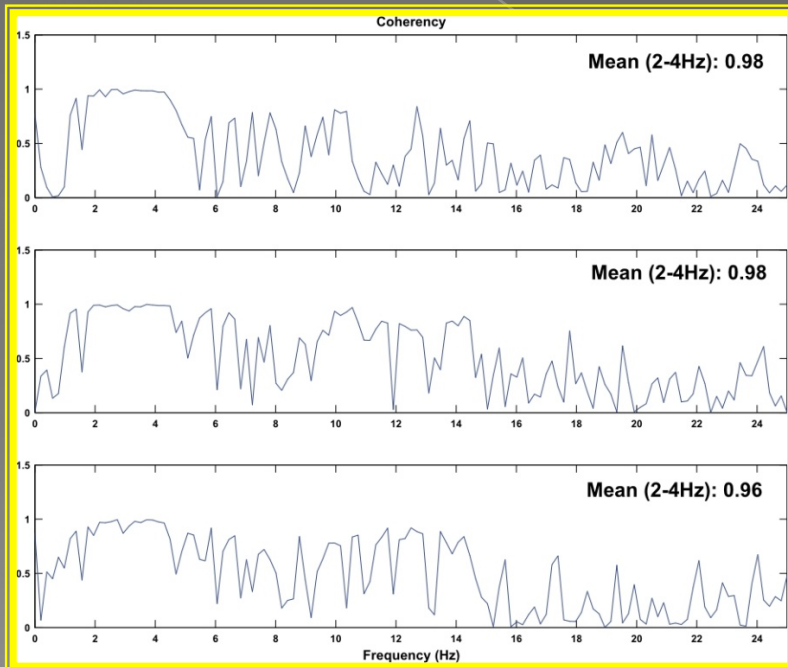
(Photos: Soto and Ruiz, 2010)



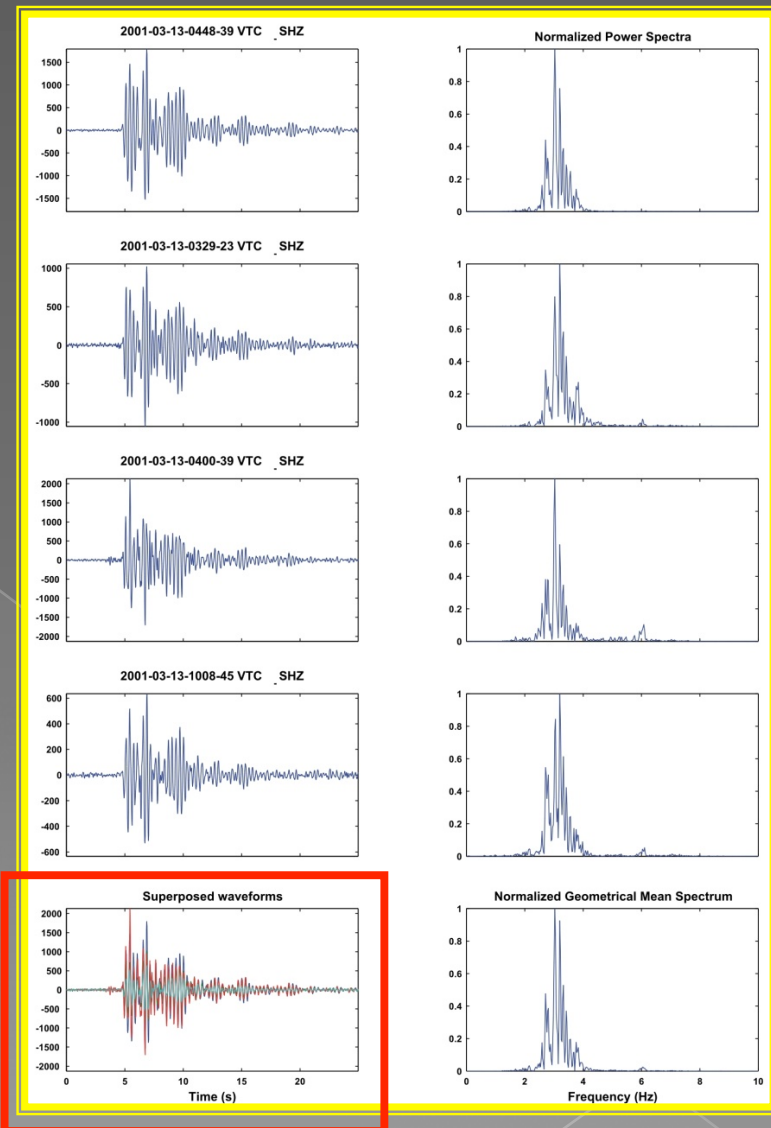
(Photos: Ruiz, 2010)

2001:

Coherency of the signals:

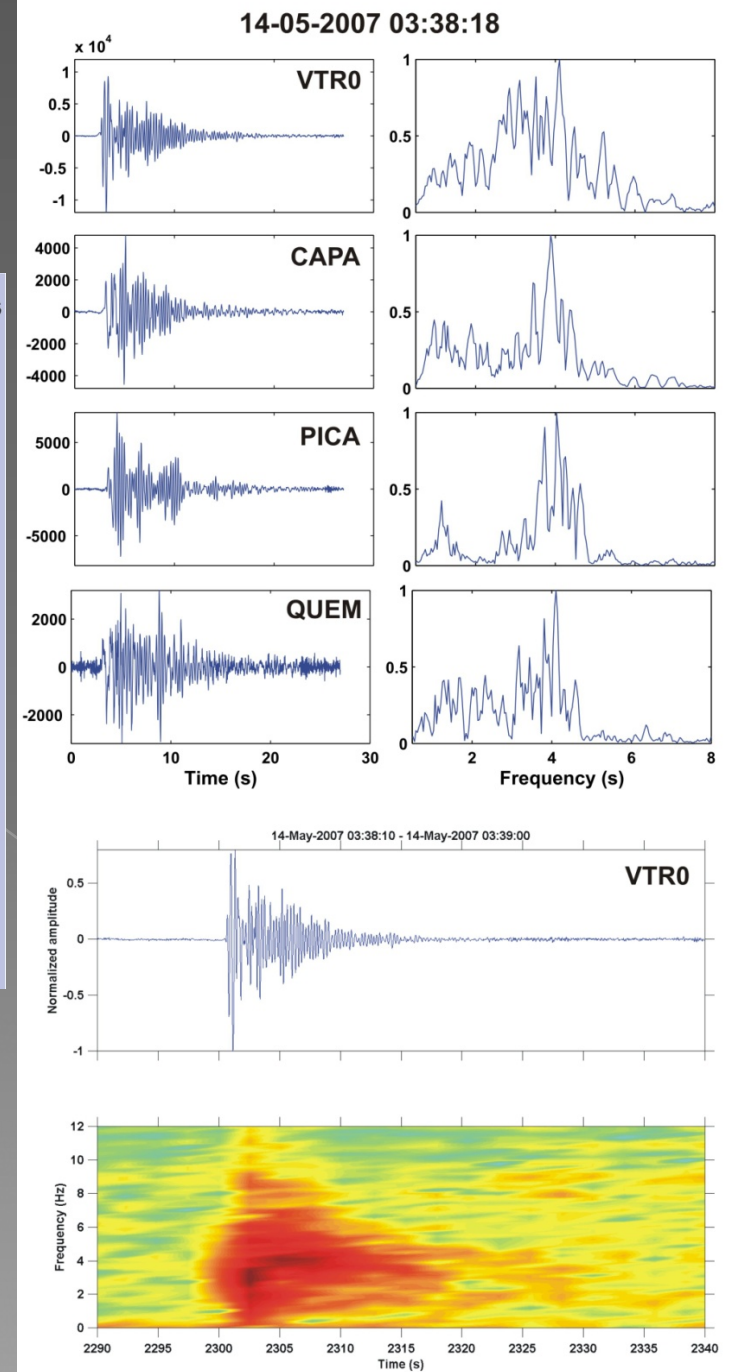
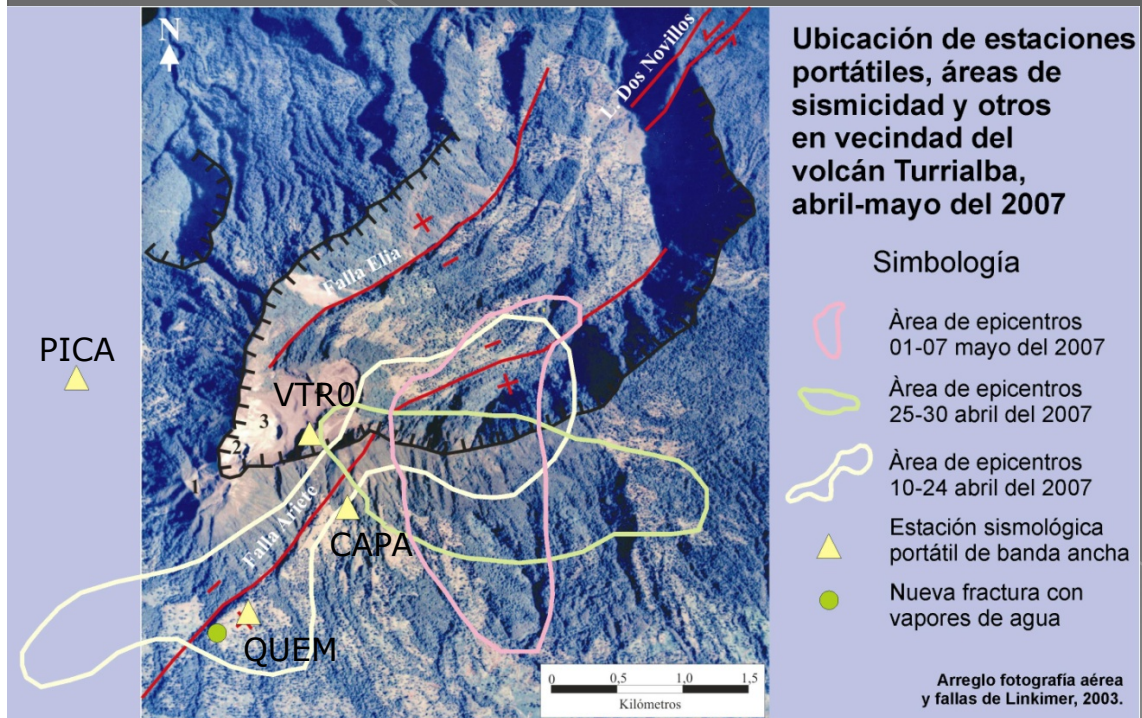


Common source



Superposed signals

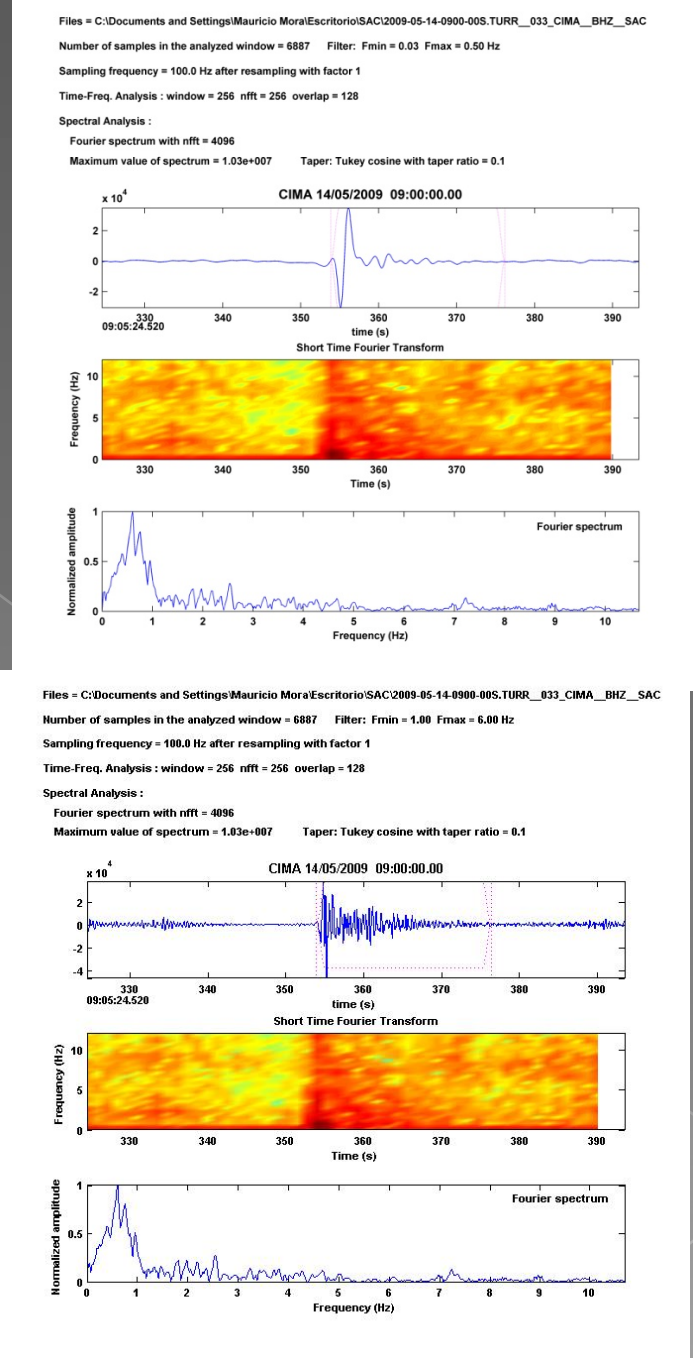
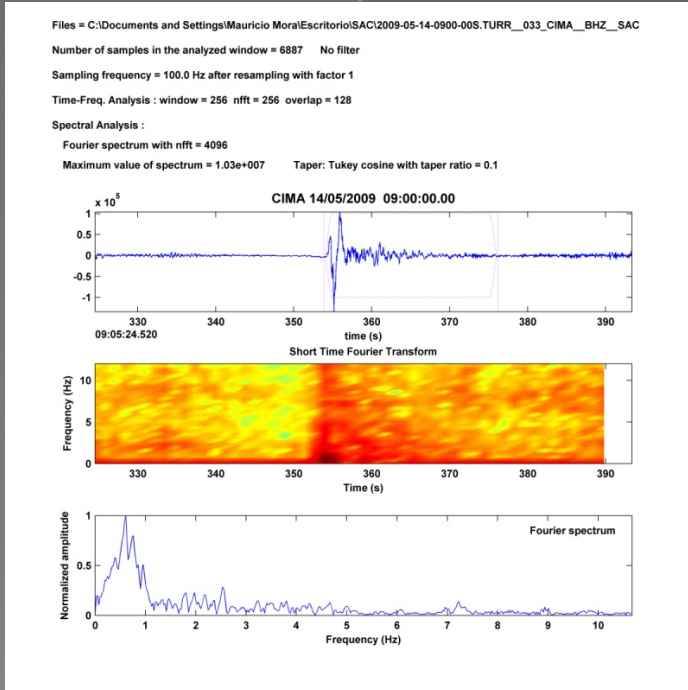
Example from Turrialba Volcano, Costa Rica (2007)

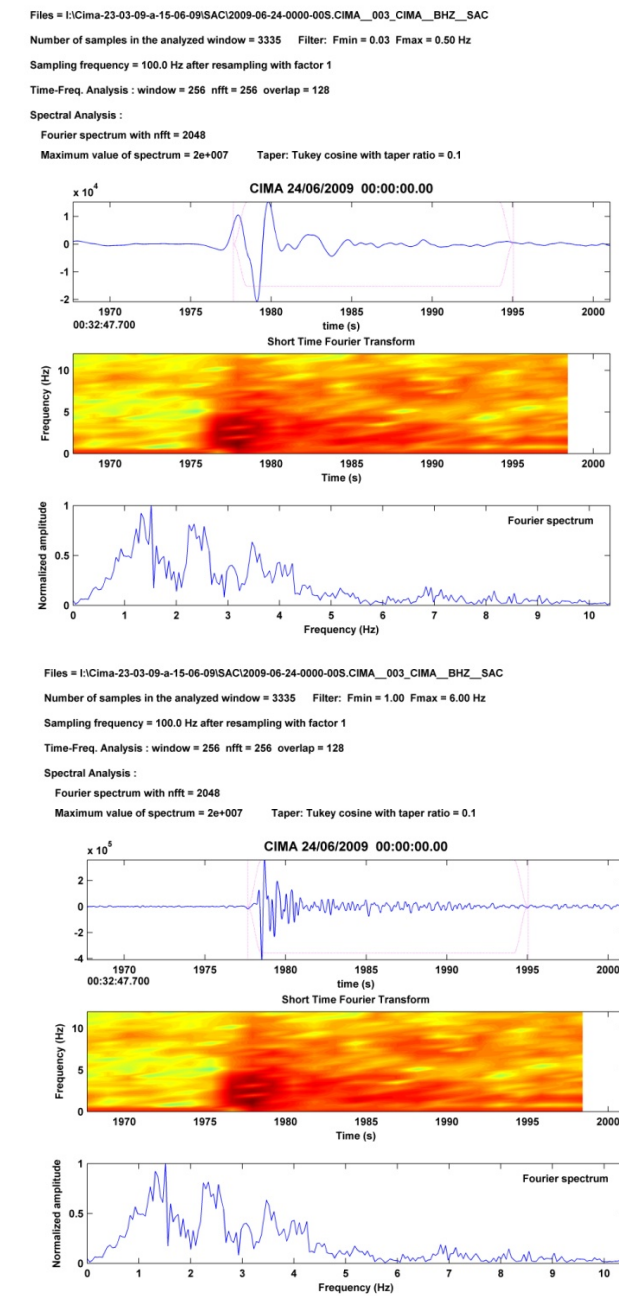
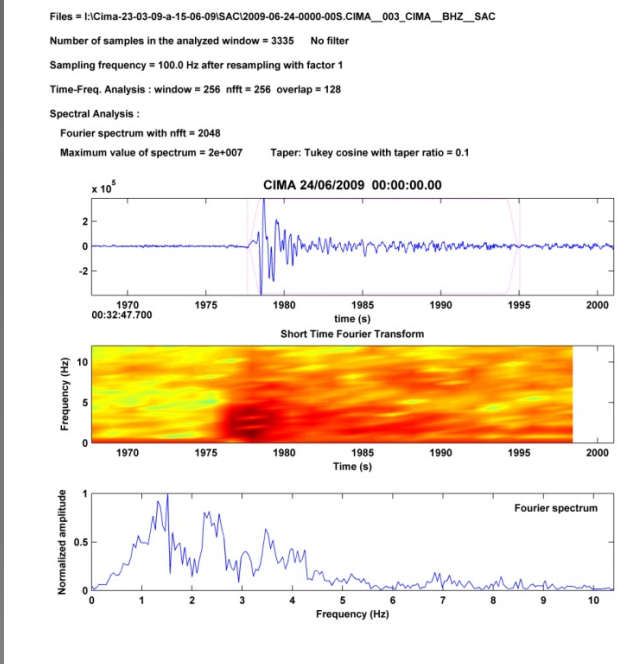


TURRIALBA VOLCANO

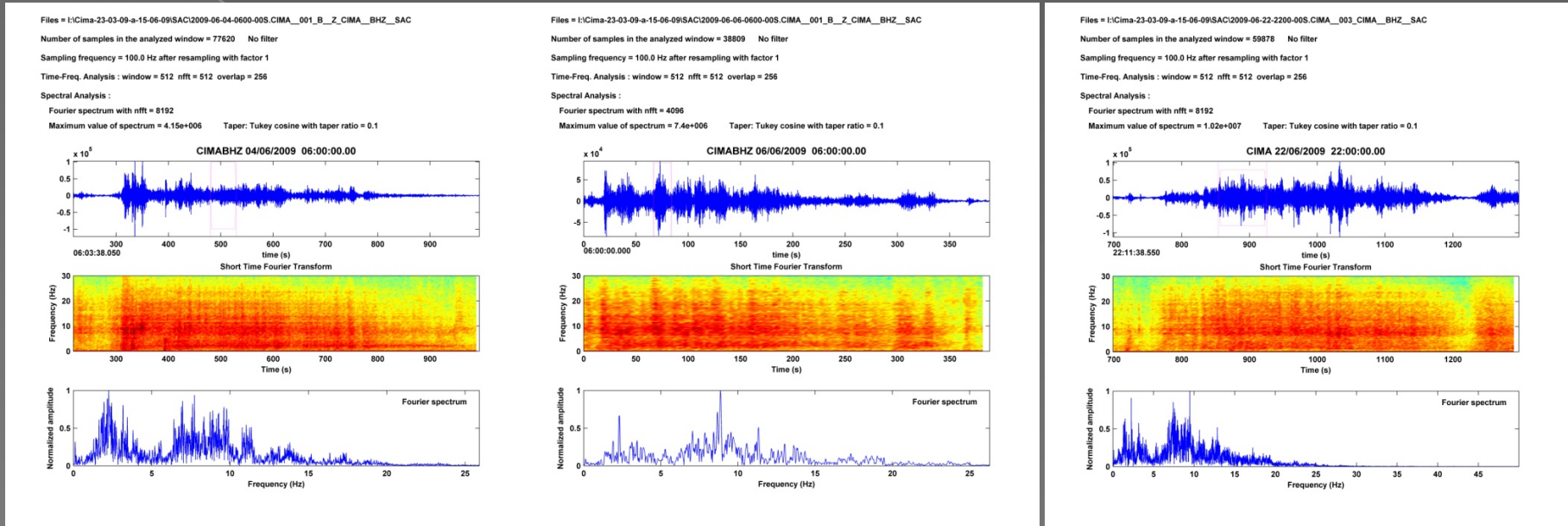
UNREST

2009...

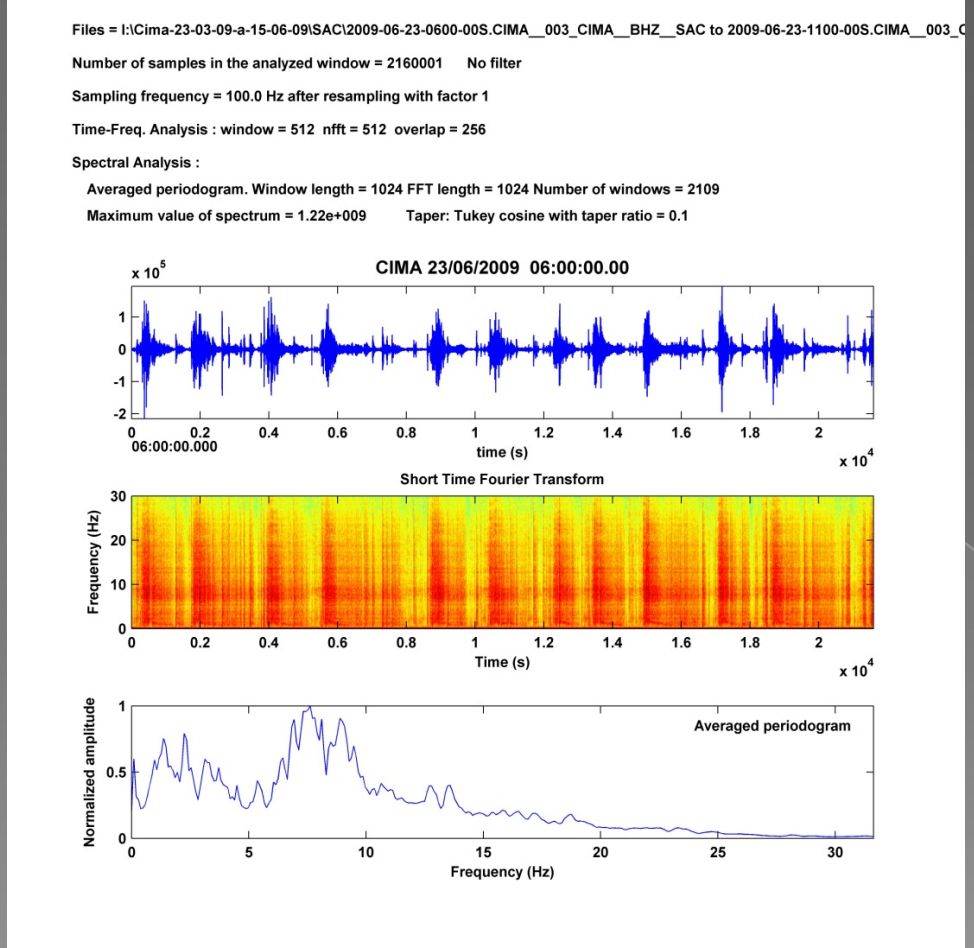




TREMOR VOLCANICO:



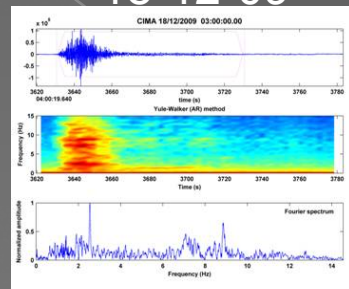
1. Frequencies around 2,5 Hz.
2. No changes on frequencies
3. Amplitude changes.



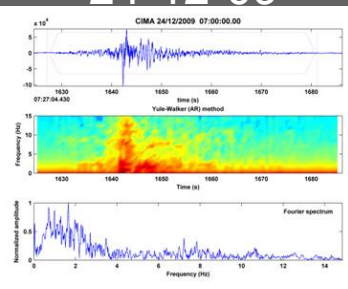
6 hours record at CIMA station.
 Tremor pulses of 10 min.

January 5th activity

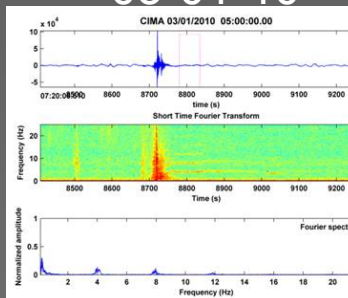
18-12-09



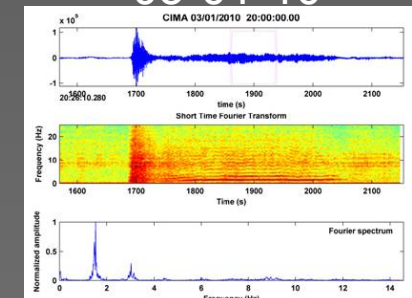
24-12-09



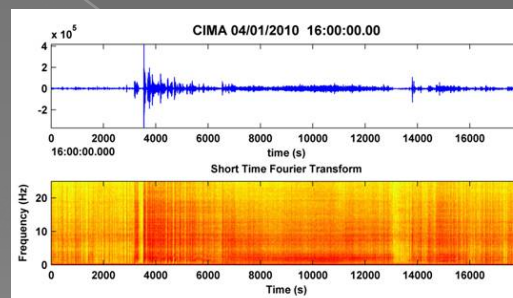
03-01-10



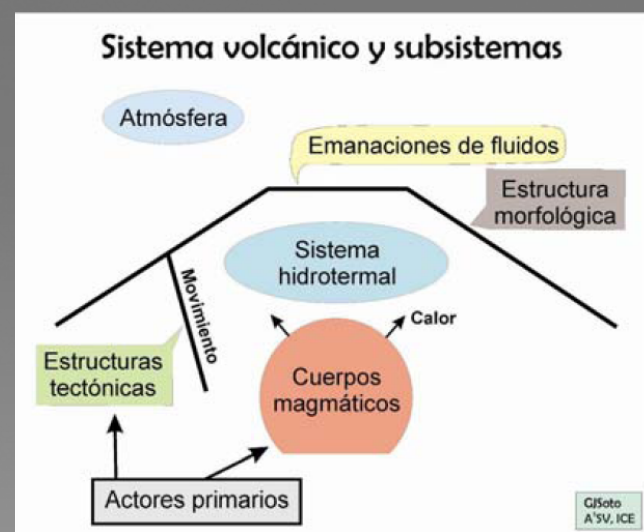
03-01-10



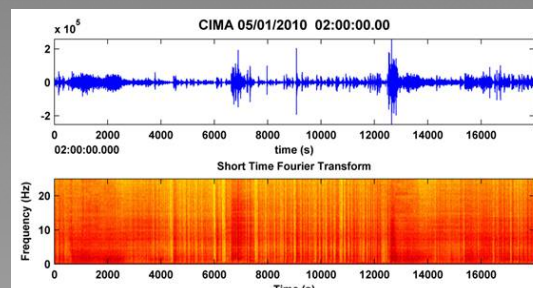
04-01-10



Eruptive process

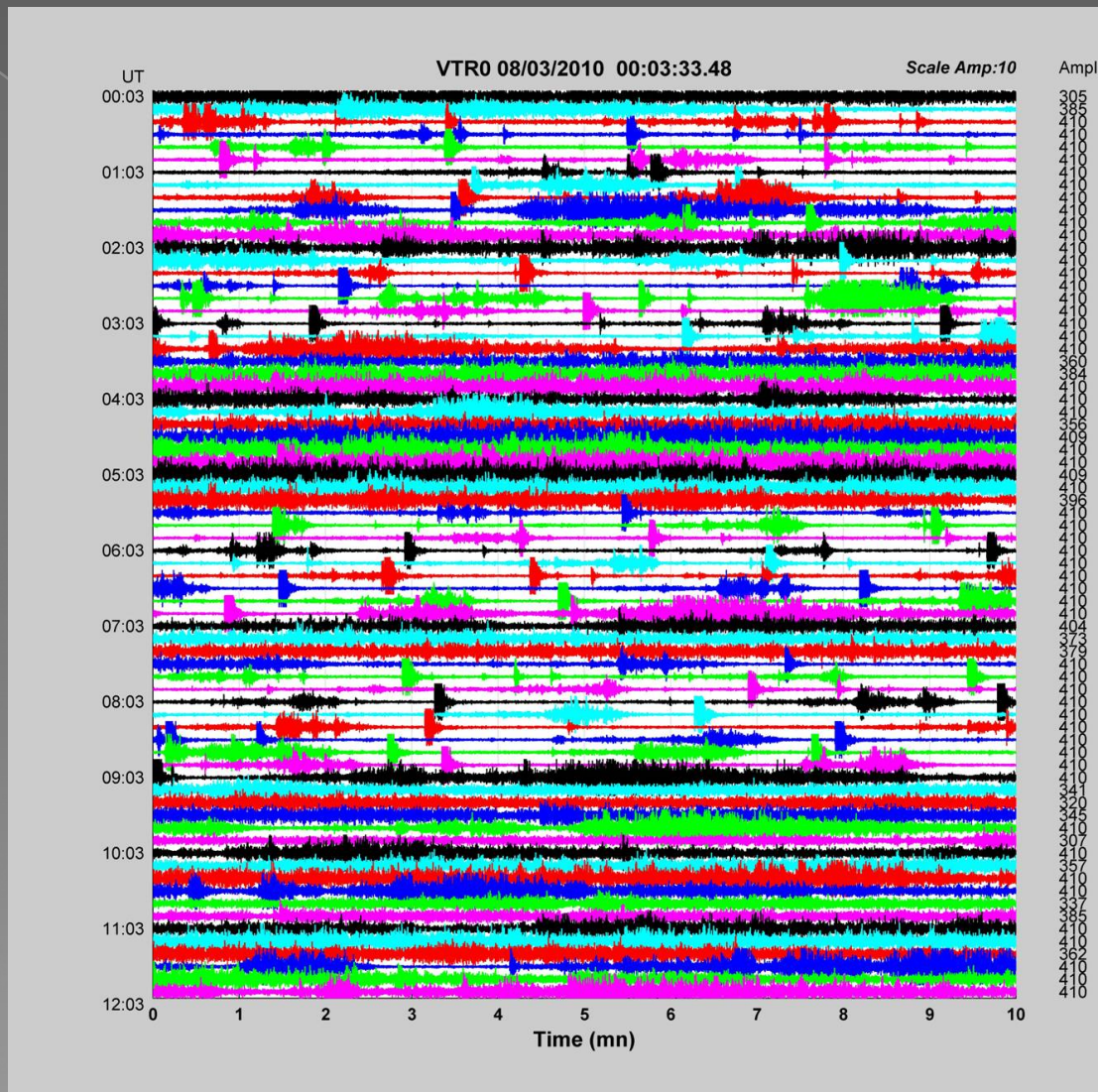


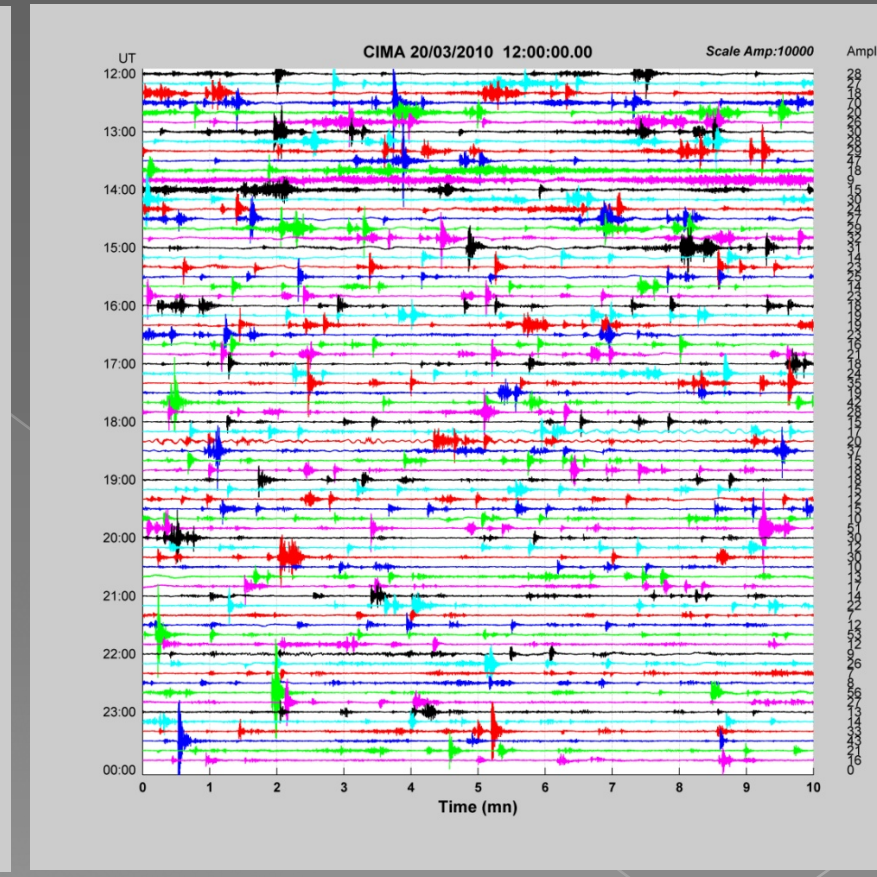
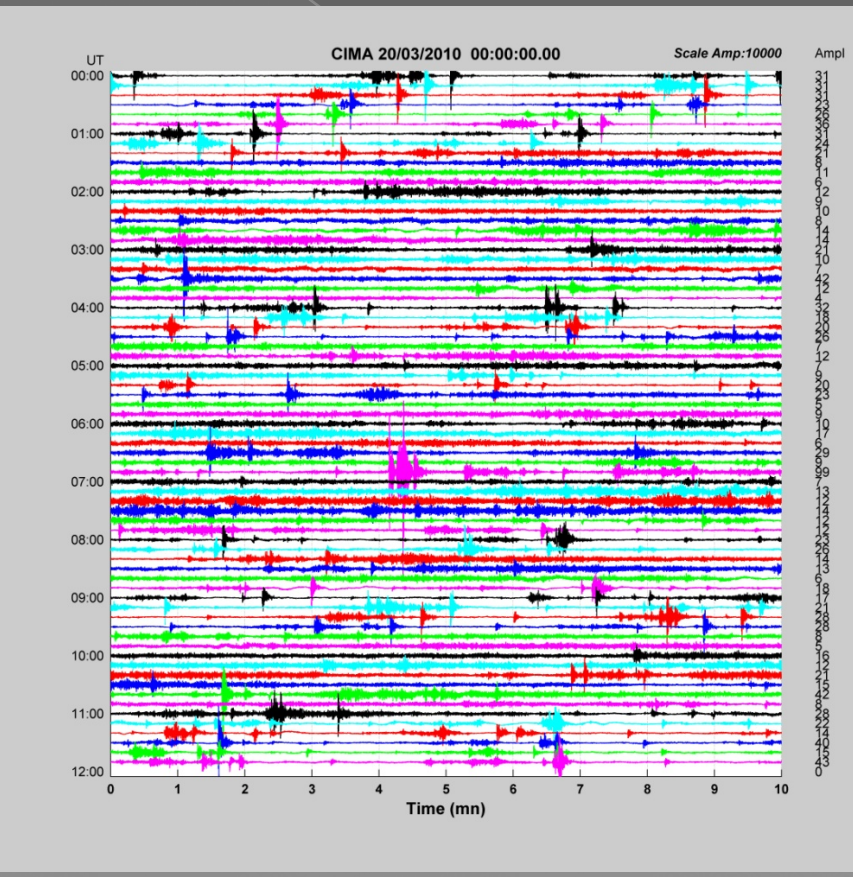
05-01-10



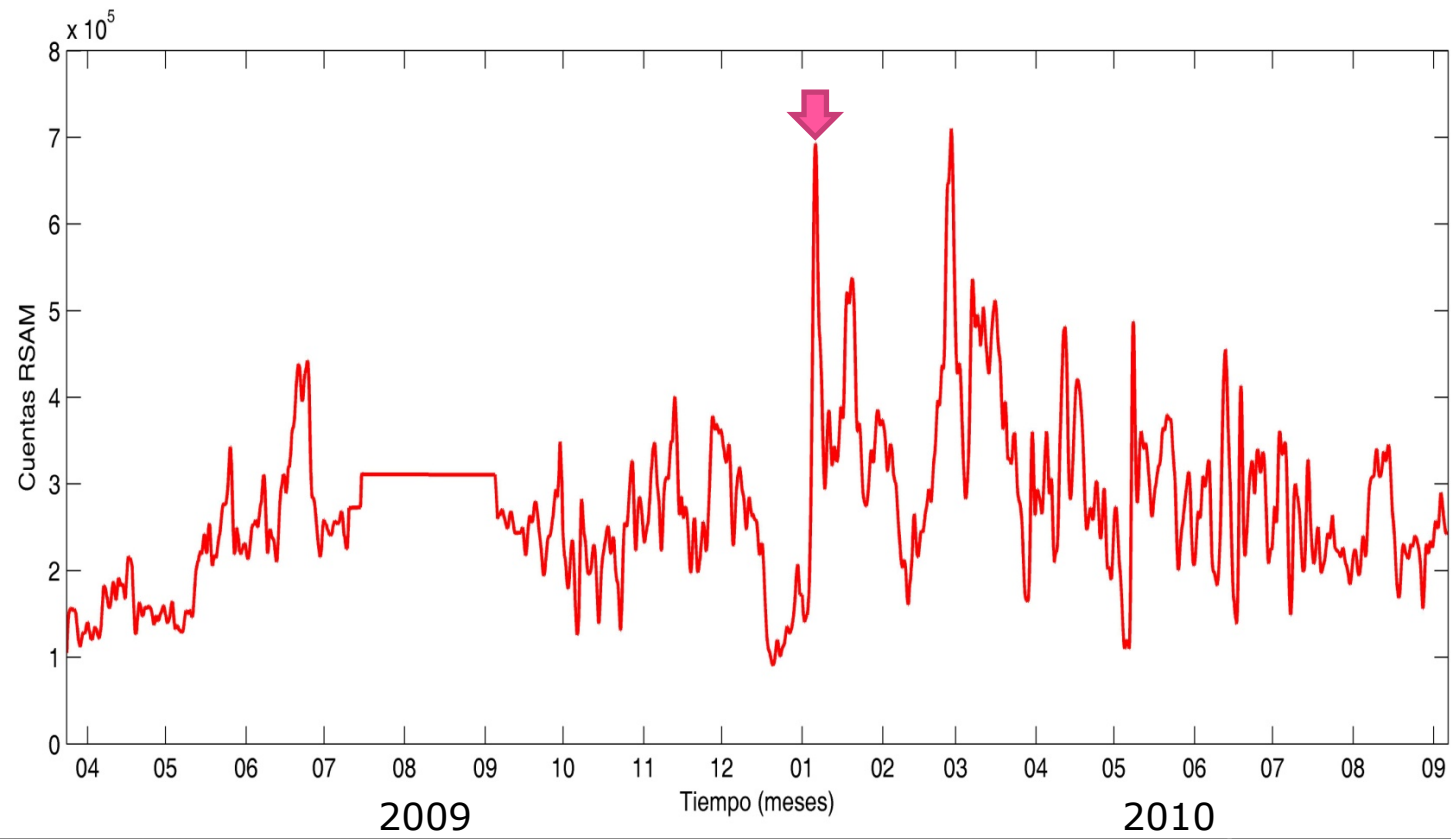


Drumbeat events (VLP events)???? March 2010





Turrialba volcano RSAM



Mapa de sismicidad de los volcanes Irazú y Turrialba (Seleccionados 2010)

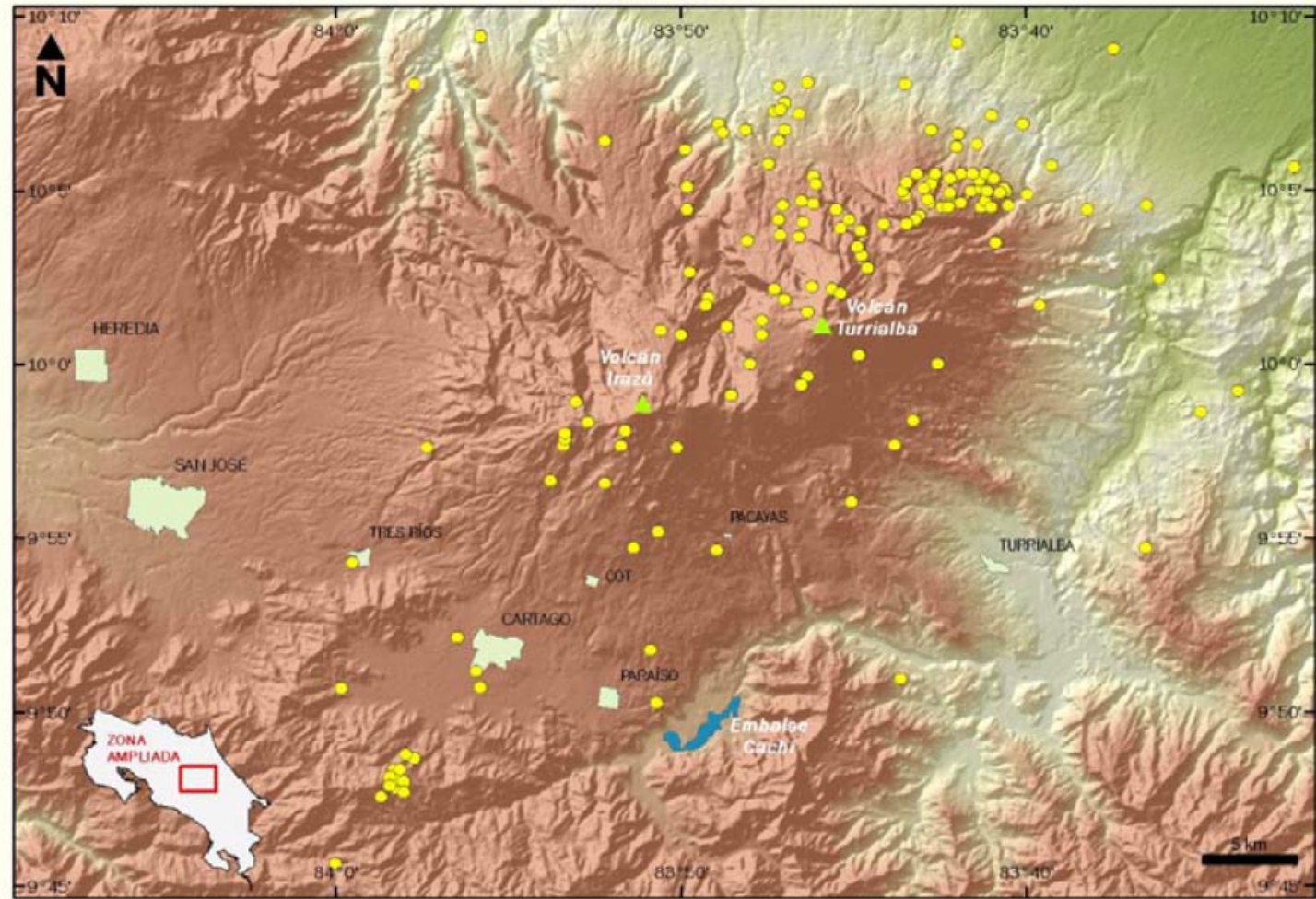


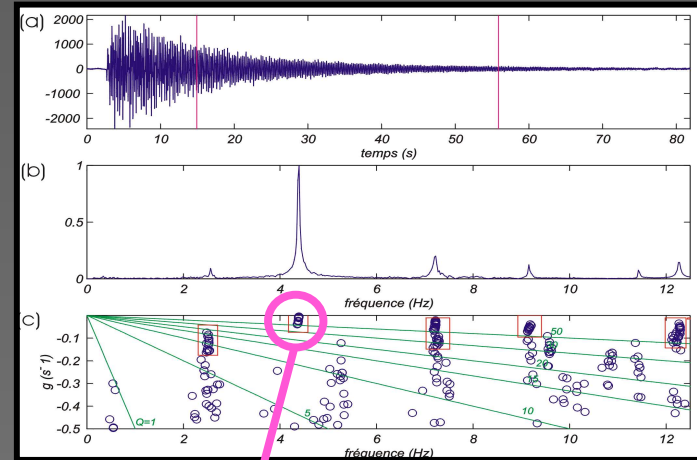
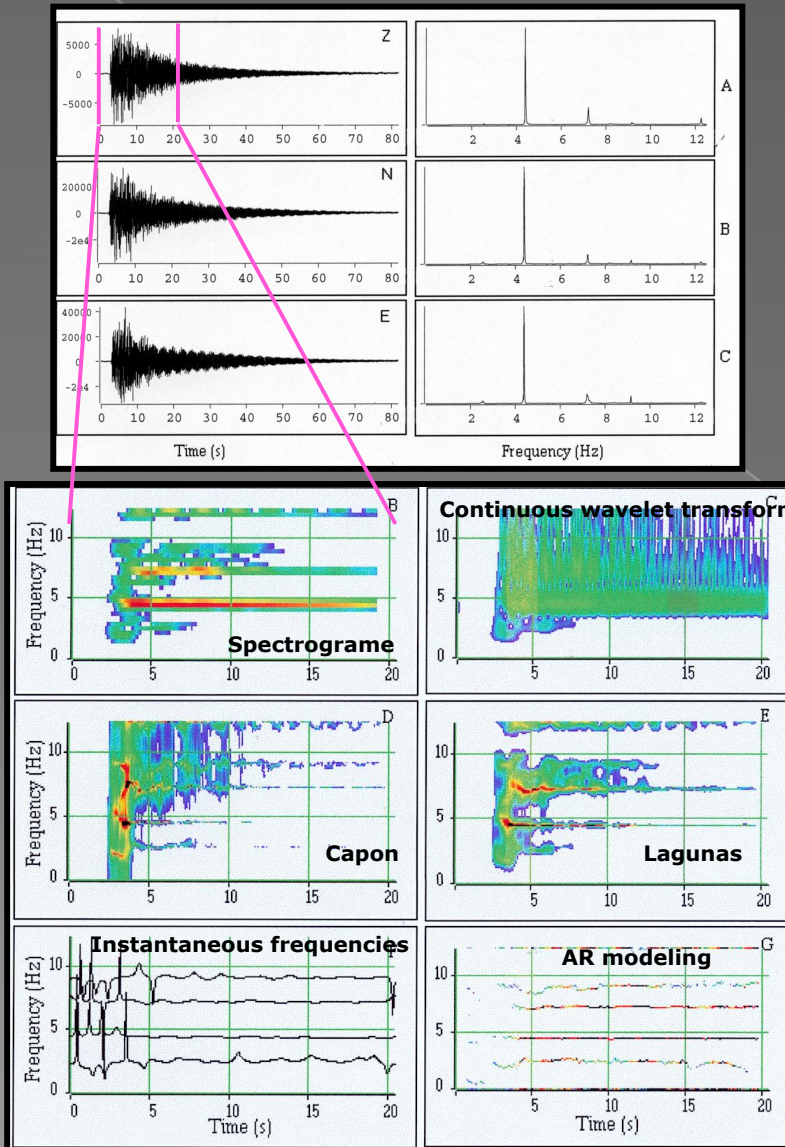
Fig. 10: Actividad sísmica en la zona Irazú-Turrialba en el 2010 (R. Barquero).

COMPARATIVE STUDIES OF DIFFERENT VOLCANOES

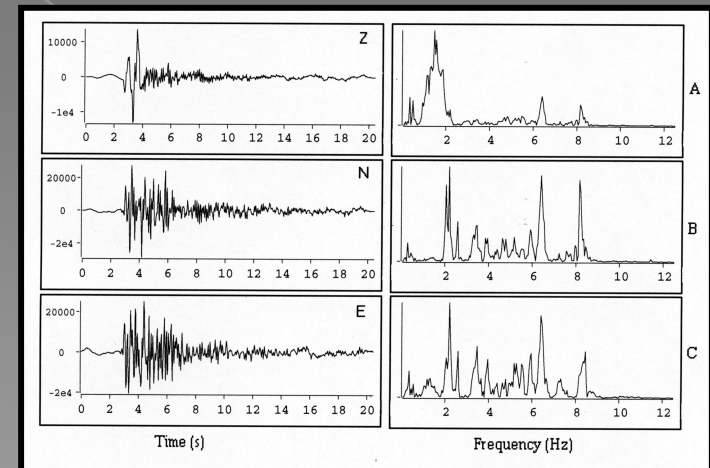
MORA (in prep.)

Time-frequency analysis of the vertical component of the LP event at Misti.

Lesage et al (2002)



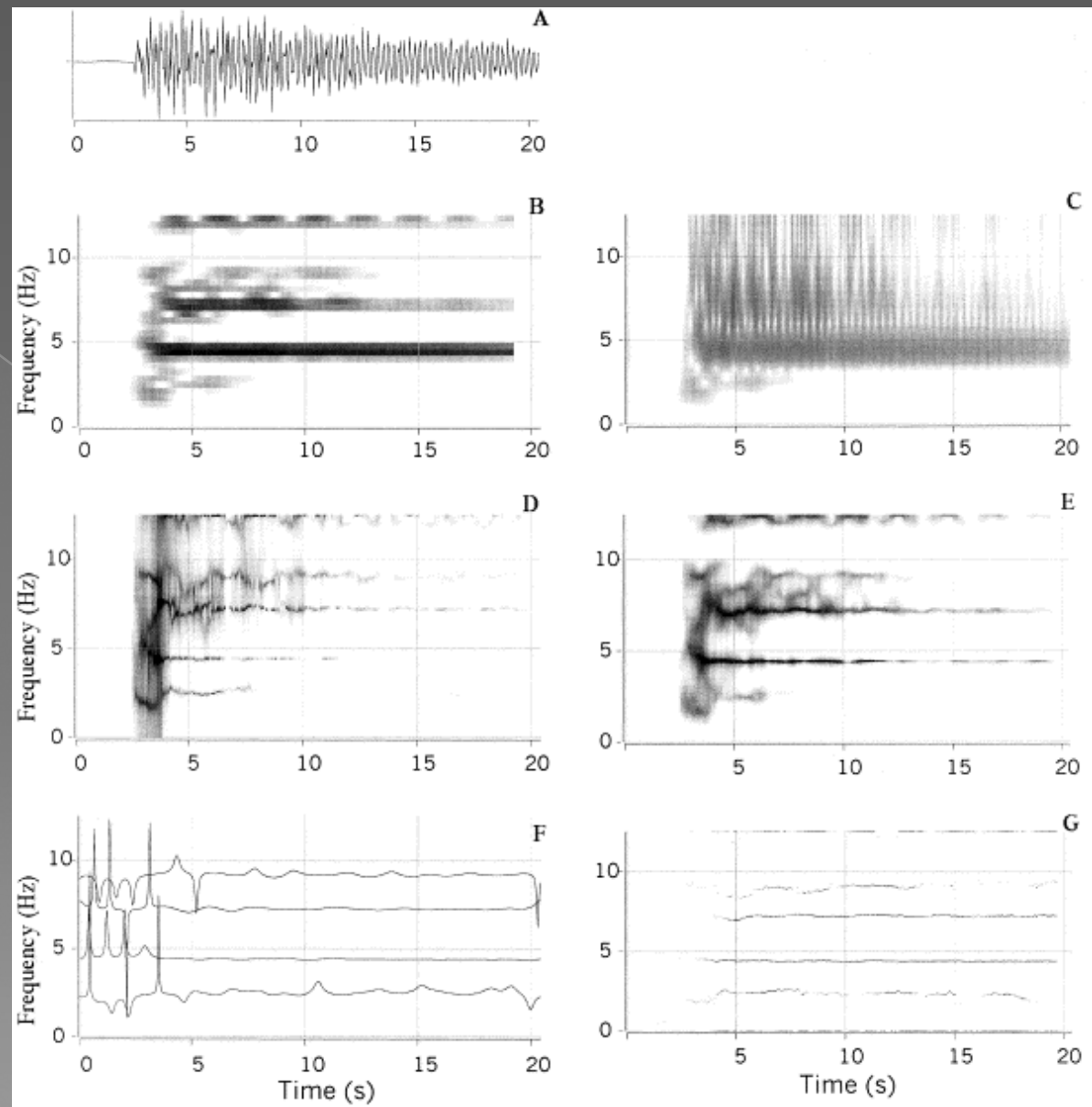
$f = 4.4 \text{ Hz}$ $Q = 210$



Deconvolution of the
signal

Time-frequency analysis of the vertical component of the LP event at Misti. (A) First 20.5 s of record. (B) STFT (2.56 s). (C) CWT. (D) Capon's method (0.6 s). (E) Lagunas method (0.8 s). (F) Instantaneous frequencies in spectral bands centered at 2.5, 4.4, 7.2, and 9.2 Hz. (G) AR modeling (0.8 s).

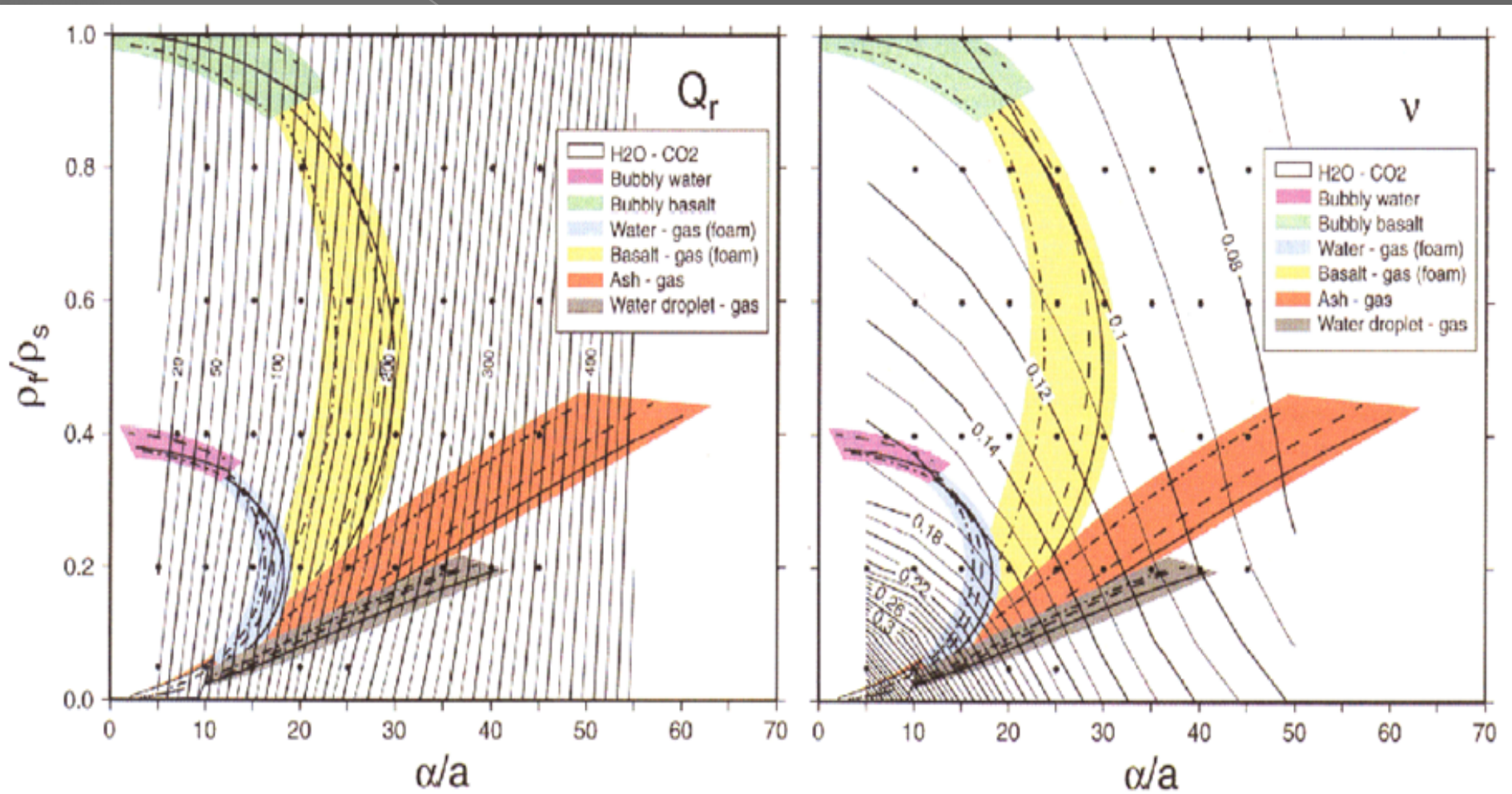
Lesage et al (2002)



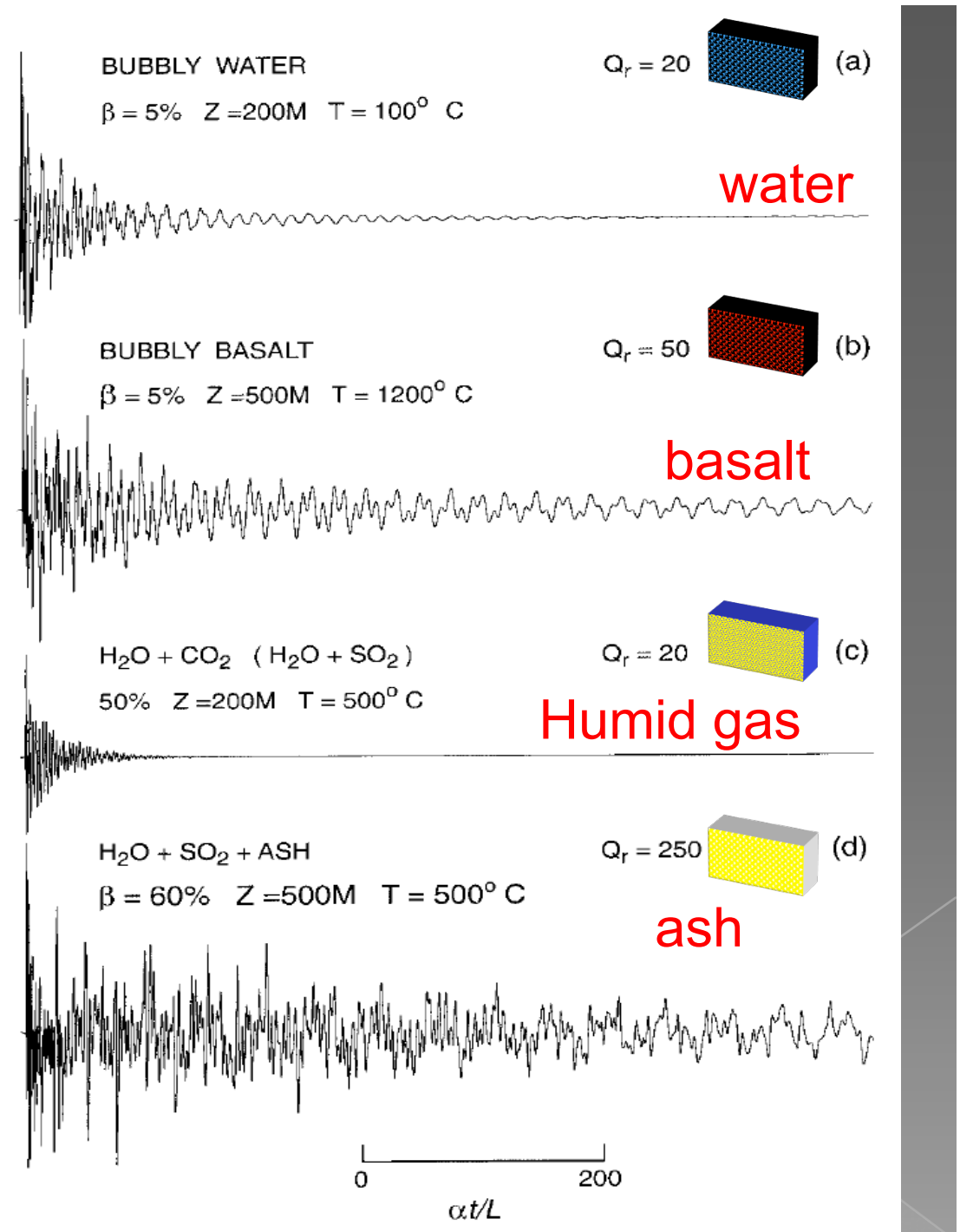
AR analysis

Each fluid has properties (compressibility, density, sound wave velocity, etc) that determine the characteristics of long period events and tremors.

Q factor analysis approach from Kumagai and Chouet (2001):

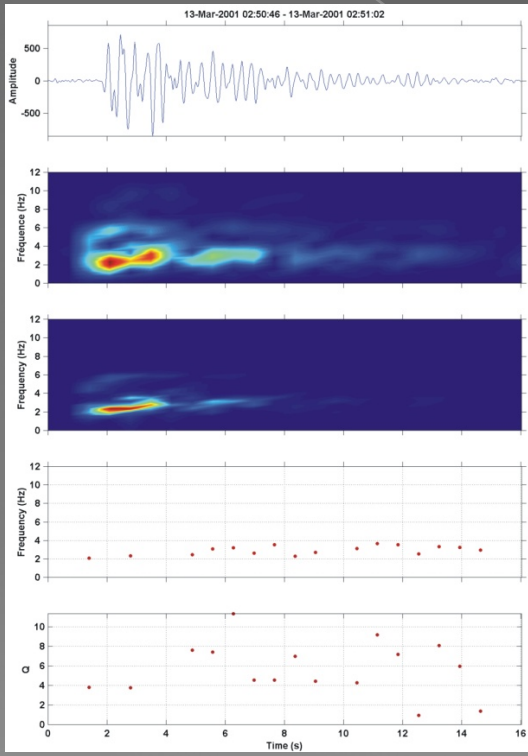


Example: Synthetic LP events calculated using a crack model filled with different kinds of volcanic fluids. (From Chouet).

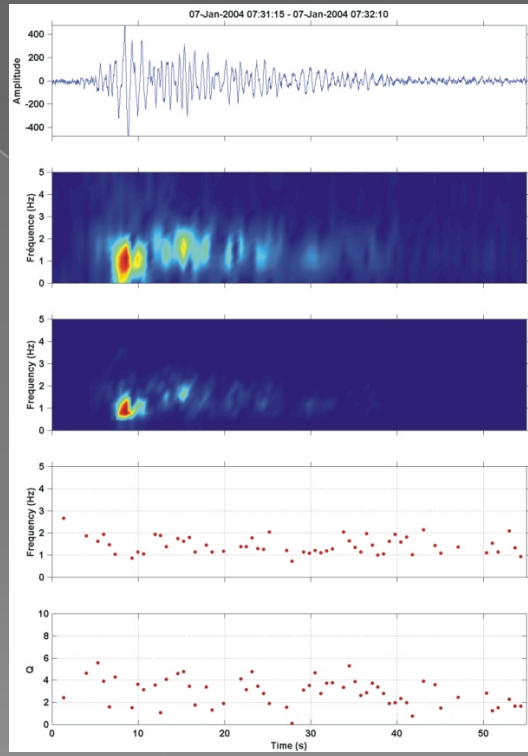


AR analysis

Turrialba



Irazu



Poas

